Molecular Therapy
Original Article

Glycine Enhances Satellite Cell Proliferation, Cell Transplantation, and Oligonucleotide Efficacy in Dystrophic Muscle

Caorui Lin,[1,5] Gang Han,[2,5] Hanhan Ning,[1] Jun Song,[1] Ning Ran,[1] Xianfu Yi,[3] Yiqi Seow,[4] and HaiFang Yin[1]

[1]Tianjin Key Laboratory of Cellular Homeostasis and Human Diseases, Department of Cell Biology, Tianjin Medical University, Qixiangtai Road, Heping District, Tianjin 300070, China; [2]School of Medical Laboratory, Tianjin Medical University, Guangdong Road, Tianjin 300203, China; [3]School of Biomedical Engineering, Tianjin Medical University, Tianjin, China; [4]Molecular Engineering Laboratory, Biomedical Sciences Institutes, Agency for Science Technology and Research, 61 Biopolis Way, Singapore 138668, Singapore

The need to distribute therapy evenly systemically throughout the large muscle volume within the body makes Duchenne muscular dystrophy (DMD) therapy a challenge. Cell and exon-skipping therapies are promising but have limited effects, and thus enhancing their therapeutic potency is of paramount importance to increase the accessibility of these therapies to DMD patients. In this study, we demonstrate that co-administered glycine improves phosphorodiamidate morpholino oligomer (PMO) potency in *mdx* mice with marked functional improvement and an up to 50-fold increase of dystrophin in abdominal muscles compared to PMO in saline. Glycine boosts satellite cell proliferation and muscle regeneration by increasing activation of mammalian target of rapamycin complex 1 (mTORC1) and replenishing the one-carbon unit pool. The expanded regenerating myofiber population then results in increased PMO uptake. Glycine also augments the transplantation efficiency of exogenous satellite cells and primary myoblasts in *mdx* mice. Our data provide evidence that glycine enhances satellite cell proliferation, cell transplantation, and oligonucleotide efficacy in *mdx* mice, and thus it has therapeutic utility for cell therapy and drug delivery in muscle-wasting diseases.

INTRODUCTION

Treating muscle disorders is a daunting challenge due to the large muscle volume. The predominant systemic muscle wasting disease, Duchenne muscular dystrophy (DMD), is caused by frame-disrupting mutations in the *DMD* gene, resulting in the absence of functional dystrophin protein.[1] The first antisense oligonucleotide (AO) drug (Exondys 51) was approved by the US Food and Drug Administration (FDA) in 2016, and it can be applied to 17.5% of DMD populations.[2] However, the therapeutic potency of this AO drug is inadequate for widespread clinical utilization, which is largely attributed to inefficient biodistribution to body-wide muscles upon systemic administration.[3] Similarly, cell therapy is another promising therapeutic modality, but it has limited efficacy due to low transplantation efficiency.[4] Therefore, strategies to enhance the efficacy of cell and exon-skipping therapies can truly improve clinical access of muscle-wasting therapies.

Amino acids are important building blocks of protein and potent regulators of protein synthesis in healthy skeletal muscle and muscle-wasting conditions.[5–8] Essential amino acids have been shown to stimulate the net muscle protein balance in healthy volunteers after resistance exercise,[9] with branched-chain amino acids having been demonstrated to alleviate muscle pathologies in DMD mice.[10] In addition, the abundance of essential amino acids within the local environment has clearly been demonstrated to trigger the activation of mammalian target of rapamycin complex 1 (mTORC1) and consequently promote protein synthesis and cell growth.[11] Recently, nonessential amino acids have also drawn much attention as food supplementation or activators of mTORC1 in preventing muscle loss.[12–15] In particular, glycine supplementation was indicated to protect muscles in different muscle-wasting models such as cancer cachexia, sepsis, and reduced caloric intake.[6,16,17] Earlier studies also demonstrated that dietary supplementation of glycine to DMD patients provided beneficial effect on their physical activities, although the overall effect is limited.[18] However, an interesting observation from earlier clinical studies was that glycine is more beneficial for children than adult patients,[18] implying that glycine might play other roles.

In this study, we show that repeated co-administration of glycine with phosphorodiamidate morpholino oligomer (PMO) increased dystrophin expression 50-fold in peripheral muscles of *mdx* mice compared to PMO in saline (PMO-S). Therapeutic levels of dystrophin were restored in *mdx* mice treated with a low dose of PMO (25 mg/kg) in glycine with marked functional improvement in the absence of detectable toxicity. This improvement can be attributed to increased uptake of PMOs in regenerating myofibers potentiated by glycine,

Received 9 January 2020; accepted 5 March 2020;
https://doi.org/10.1016/j.ymthe.2020.03.003.

[5]These authors contributed equally to this work.

Correspondence: HaiFang Yin, Tianjin Key Laboratory of Cellular Homeostasis and Human Diseases, Department of Cell Biology, Tianjin Medical University, Qixiangtai Road, Heping District, Tianjin 300070, China.
E-mail: haifangyin@tmu.edu.cn

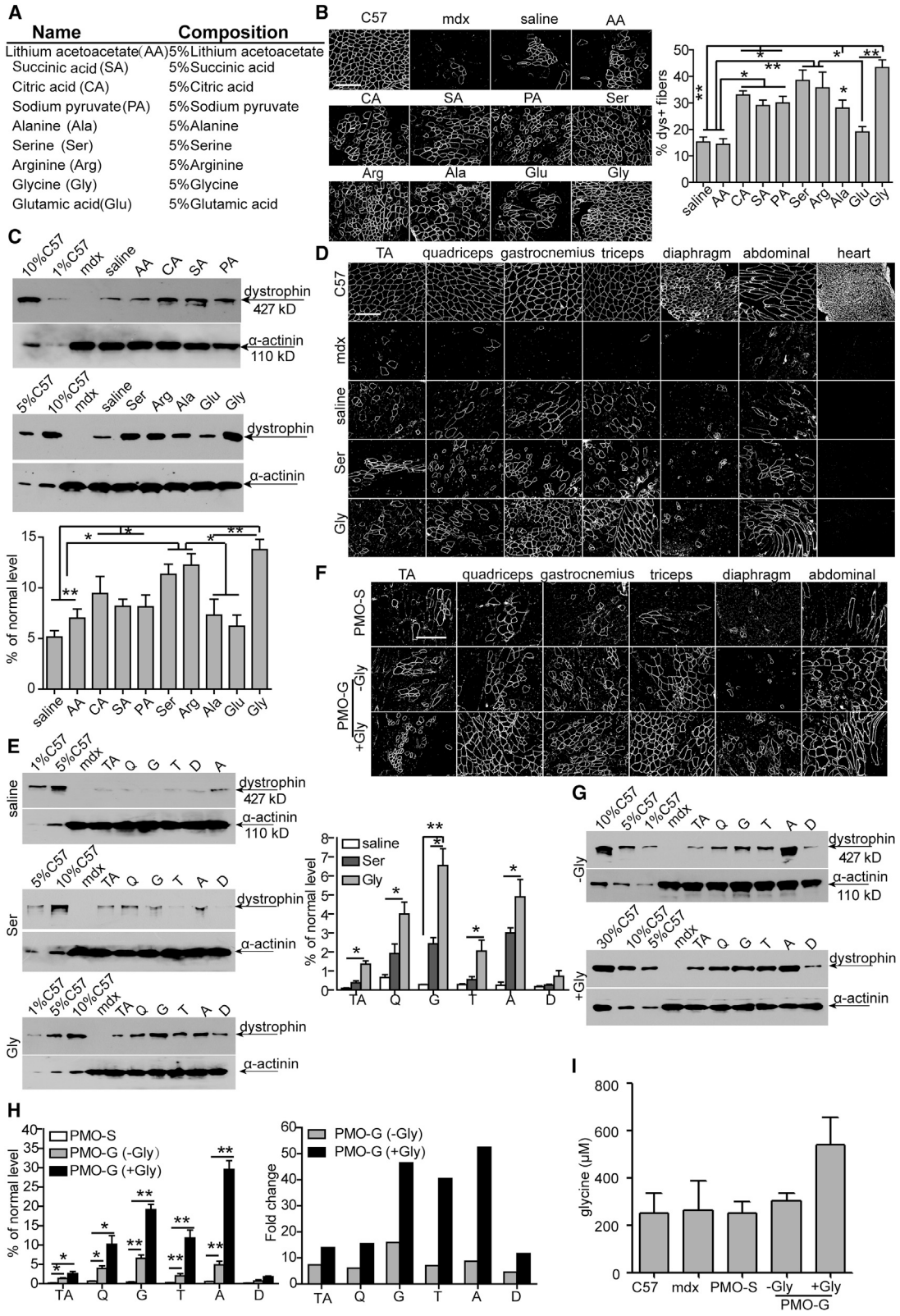

(legend on next page)

which in turn is mediated by enhanced mTORC1 activation and one-carbon unit pool replenishment. Importantly, glycine promoted not only endogenous satellite cell proliferation but also cell transplantation efficiency of exogenous satellite cells and primary myoblasts. The findings presented herein provide insights for the role of glycine and have important therapeutic implications for cell therapy and nucleic acid therapeutics in muscle-wasting diseases and other muscle-related disorders.

RESULTS

Glycine Enhances PMO-Mediated Exon Skipping in Muscle

As hexose was shown to promote the uptake and activity of PMO in peripheral muscles of *mdx* mice by replenishing cellular energy stores,[19] we examined whether other nutrients could similarly improve PMO-mediated exon skipping in dystrophic muscles (Figure 1A). Unsurprisingly, consistent with previous observations with hexose,[19] alternative energy sources such as citric acid, sodium pyruvate, and succinic acid induced improvements in PMO activities as reflected by significantly increased dystrophin-positive fibers and levels of dystrophin restoration in tibialis anterior (TA) muscles from *mdx* mice treated with PMO in citric acid, sodium pyruvate, and succinic acid compared to PMO in saline (Figure 1B). However, it was surprising that amino acids, particularly serine and glycine, induced a significant increase in PMO-induced dystrophin-positive fibers (Figure 1B) and dystrophin expression (Figure 1C) in TA muscles of treated *mdx* mice. To determine the systemic effect of glycine and serine on PMO activity, we intravenously administered 5% glycine (equivalent to clinically available 50 mg/mL infusion buffer) or serine with PMO at the dose of 25 mg/kg/week for 3 weeks in *mdx* mice. Substantial numbers of dystrophin-positive myofibers (Figure 1D) and significantly elevated levels of dystrophin (Figure 1E) were detected in most peripheral muscles of *mdx* mice treated with PMO in glycine (PMO-G) compared to PMO in serine and PMO-S. To examine whether there is any dose-dependent effect for PMO or glycine, we increased the dose of PMO from 25 to 50 mg/kg/week for 3 weeks or the administration frequency of glycine from weekly to every other day for 5 weeks with the same dose of PMO (25 mg/kg/week) for 3 weeks. As expected, glycine also enhanced the number of dystrophin-positive fibers and dystrophin expression compared to saline when co-delivered with 50 mg/kg PMO (Figures S1A–S1C). In contrast, dystrophin-positive fibers (Figure 1F) and dystrophin expression (Figure 1G) dramatically rose in peripheral muscles of PMO-G-treated *mdx* mice with additional glycine infusion compared to PMO-G alone. Importantly, up to a 50-fold higher level of dystrophin was detected in abdominal muscles from *mdx* mice treated with PMO-G with additional glycine administration compared to PMO-S under identical conditions (Figure 1H). Measurement of serum glycine revealed slightly higher levels after infusion with additional glycine than PMO-G alone (Figure 1I), suggesting that increased glycine availability enhances PMO-mediated exon skipping. However, increasing glycine from 5% to 10% did not improve PMO activity (Figures S1D and S1E), implying that the effect is saturable. The fact that increased glycine concentration at the point of injection did not improve uptake, but increased the frequency of administration, suggests that the improvements seen in mice are not solely due to short-lived effects such as increasing uptake of circulating PMO. These data demonstrate that glycine potentiates PMO activities in muscle, and the potentiating effect can be enhanced by a sustained supply of glycine.

PMO-G Elicits Long-Term Efficacy and Functional Improvements in *mdx* Mice

Since PMO-G with additional glycine infusion further enhanced PMO activities in *mdx* mice, we adopted this dosing regimen at 25 mg/kg PMO for a period of 6 months (Figure 2A). Repeated administration of PMO-G induced uniform dystrophin expression

Figure 1. Screening of Amino Acids with PMO in Adult *mdx* Mice

(A) Different concentrations of nutrients used for the study. (B–E) Dystrophin expression following single intramuscular injection of 2 μg of PMO into *mdx* TA muscles (B and C) or intravenous injection of PMO at 25 mg/kg/week for 3 weeks in different amino acid solutions or saline in *mdx* mice, respectively (D and E). (B) Immunohistochemistry and quantitative analysis for dystrophin-positive fibers in *mdx* TA muscles treated with single intramuscular injection of 2 μg of PMO in different nutrients (scale bar, 100 μm). The concentration was 5%, as illustrated in (A). For glycine and saline groups, the number of animals used per group is six (n = 6) and the rest is three (n = 3; one-way ANOVA and *post hoc* Student-Newman-Keuls test). White staining on fiber membrane shows dystrophin expression. (C) Representative western blot and quantitative analysis for dystrophin expression in TA muscles from *mdx* mice treated with single intramuscular injection of PMO in different solutions. For glycine and saline groups, the number of animals used per group is six (n = 6) and the rest is three (n = 3; one-way ANOVA and *post hoc* Student-Newman-Keuls test). α-Actinin was used as the loading control. 5, 2.5, and 0.5 μg of total protein from *C57BL/6* mice and 50 μg from muscle samples from untreated and treated *mdx* mice were loaded. TA muscles from *C57BL/6* mice were used as normal controls (the same is true for all western blots unless otherwise specified). (D) Immunohistochemistry for dystrophin expression in body-wide muscles from *mdx* mice treated intravenously with PMO in saline or amino acid solutions (5%) at 25 mg/kg/week for 3 weeks. TA, tibialis anterior. Scale bar, 100 μm. (E) Western blot and quantitative analysis of dystrophin expression in body-wide muscles from *mdx* mice treated intravenously with PMO in glycine (n = 4), serine, or saline (n = 3) at 25 mg/kg/week for 3 weeks (one-way ANOVA and *post hoc* Student-Newman-Keuls test). 0.5, 2.5, and 5 μg of total protein from *C57BL/6* mice and 50 μg from muscle samples from untreated and treated *mdx* mice were loaded. (F) Immunohistochemistry for dystrophin expression in body-wide muscles from *mdx* mice treated intravenously with PMO in glycine at 25 mg/kg/week for 3 weeks with glycine (+Gly) or without additional glycine (−Gly) every other day for 5 weeks (scale bar, 100 μm). (G) Western blot for dystrophin expression in body-wide muscles from *mdx* mice treated intravenously with PMO in glycine at 25 mg/kg/week for 3 weeks with glycine (+Gly) or without additional glycine (−Gly) every other day for 5 weeks. 0.5, 2.5, 5, and 15 μg of total protein from *C57BL/6* mice and 50 μg from muscle samples from untreated and treated *mdx* mice were loaded. TA, tibialis anterior; Q, quadriceps; G, gastrocnemius; T, triceps; A, abdominal muscle; D, diaphragm. (H) Quantitative analysis of dystrophin expression in body-wide muscles from *mdx* mice treated intravenously with PMO in glycine at 25 mg/kg/week for 3 weeks with glycine (+Gly) or without additional glycine (−Gly) every other day for 5 weeks (n = 4; one-way ANOVA and *post hoc* Student-Newman-Keuls test). (I) ELISA assay for measurement of glycine in serum from *mdx* mice treated intravenously with PMO in glycine at 25 mg/kg/week for 3 weeks with glycine (+Gly) or without additional glycine (−Gly) every other day for 5 weeks (n = 4). Data are presented as means ± SEM. $^{*}p < 0.05$, $^{**}p < 0.001$.

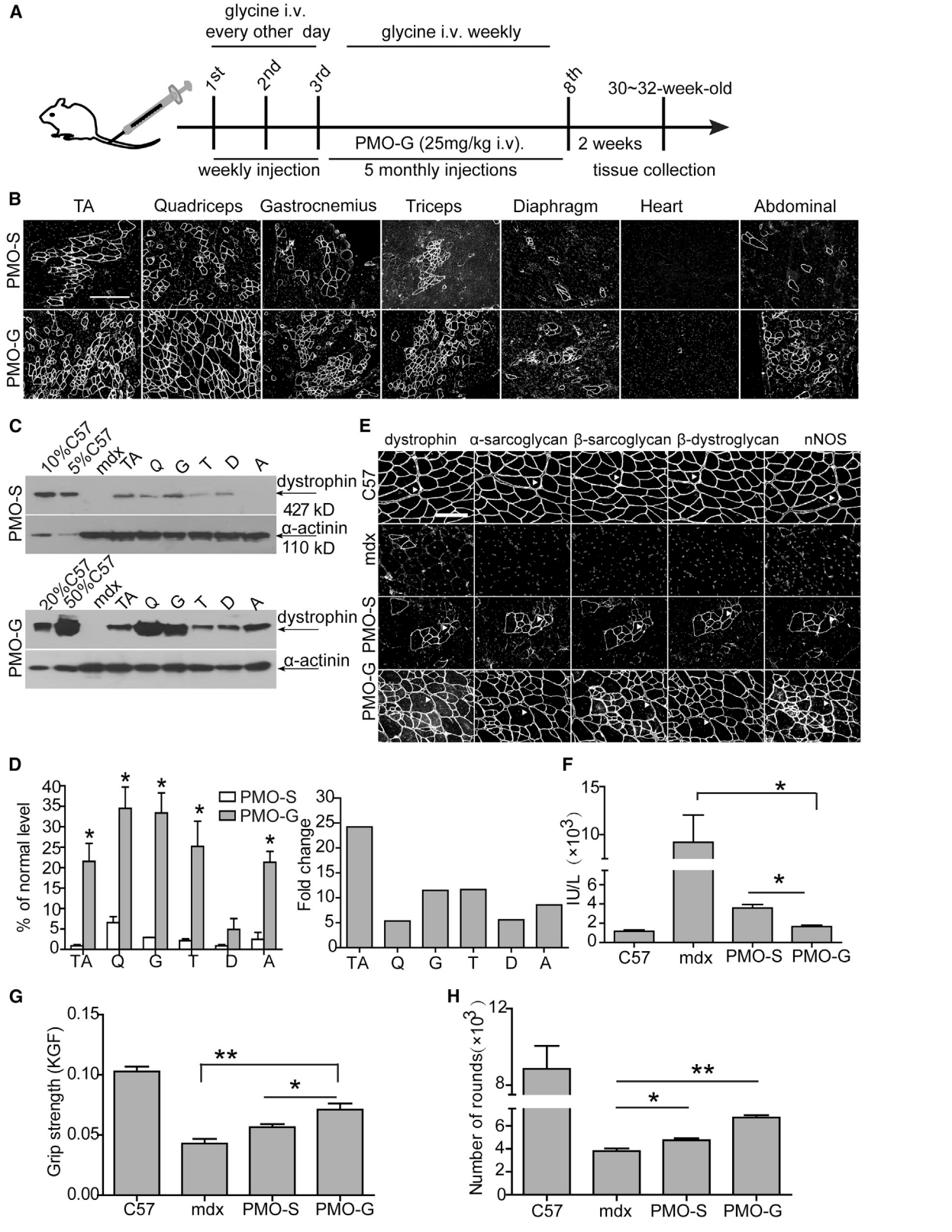

(legend on next page)

across most peripheral muscles except for diaphragm, with no dystrophin expressed in the heart (Figure 2B). Dystrophin levels were consistently elevated in peripheral muscles of PMO-G-treated *mdx* mice compared to PMO-S under identical conditions (Figures 2C and 2D). Importantly, molecular correction of dystrophin resulted in functional improvements in PMO-G-treated *mdx* mice, as dystrophin-associated protein complex (DAPC), which mis-localizes in the absence of dystrophin,[20] re-localized to the sarcolemma (Figure 2E); serum creatine kinase (CK) levels that are usually elevated in *mdx* mice[21] significantly decreased (Figure 2F); immunoglobulin G (IgG) staining also declined (Figure S2A). Significant force recovery and endurance improvements were also observed as reflected by significantly increased grip strength and the number of rounds measured with a running wheel test in *mdx* mice treated with PMO-G compared to PMO-S and untreated *mdx* mice (Figures 2G and 2H). Levels of serum aspartate aminotransferase (AST) and alanine aminotransferase (ALT) concordantly declined, whereas no change was found for creatinine and urea (Figure S2B), and histology revealed no evidence of liver or renal toxicity (Figure S2C). Strikingly, inflammatory cells and fibrosis dramatically decreased in peripheral muscles from PMO-G-treated *mdx* mice compared to PMO-S and age-matched untreated *mdx* controls (Figures S2D and S2E). Interestingly, body weight was significantly increased in PMO-G-treated *mdx* mice at earlier time points compared to PMO-S and age-matched untreated *mdx* controls, although the difference declined at later time points (Figure S2F), suggesting that glycine might have some beneficial effects on muscle growth, although the caveat is that hypertrophy observed in *mdx* mice may also increase muscle volume. These findings indicate that long-term administration of PMO-G leads to significant functional improvements in *mdx* mice at extremely low doses without any detectable toxicity.

Glycine Synergizes with PMO Therapy by Improving Muscle Regeneration, which Results in Greater PMO Uptake and Efficacy

To investigate whether the enhancement elicited by glycine was due to greater exon-skipping frequency[22] or through enhanced PMO uptake, we administered PMO (2 μg) in saline into TA muscles of adult *mdx* mice followed by injection of glycine to the same muscle 16 h later, to allow for complete uptake of PMO into the muscle prior to glycine introduction.[22] However, separating glycine from PMO negated the enhancement observed with PMO-G (Figures 3A and 3B), suggesting that glycine is involved in PMO uptake rather than enhancing exon-skipping frequency. To test whether glycine functions by increasing PMO uptake, we intravenously administered lissamine-labeled PMO in glycine into adult *mdx* mice at 25 mg/kg/day for 3 days. However, no difference was observed in the fluorescence intensity of body-wide tissues from PMO-G- and PMO-S-treated *mdx* mice 4 days after injection under identical conditions (Figure S3A). Comparable levels of adenosine triphosphate (ATP) were consistently found in quadriceps from *mdx* mice treated with PMO-G and PMO-S (Figure S3B), indicating that glycine did not increase energy availability. Since PMO-G with additional glycine infusion outperformed PMO-G alone, we re-examined the samples and noticed that significantly higher numbers of small-caliber embryonic myosin heavy chain (eMyHC)-positive[23] regenerating myofibers were present in quadriceps and triceps from PMO-G-treated *mdx* mice with additional glycine injection compared to PMO-G alone and PMO-S (Figure S3C), implying that glycine promotes muscle regeneration. Given that muscle regeneration was shown to contribute to PMO uptake in *mdx* mice,[24] we hypothesized that glycine might promote muscle regeneration and thus enhance PMO uptake. To verify this, we intravenously injected glycine into adult *mdx* mice every other day for 1 week to induce muscle regeneration, followed by single intravenous injection of carboxyfluorescein (fluorescein isothiocyanate [FITC])-labeled PMO at the dose of 50 mg/kg, and examined the uptake of PMO 48 h later. Muscle satellite cells (MuSCs), indicated by paired box transcription factor (PAX7), a known satellite cell marker,[25] and the percentage of proliferating $PAX7^{+}/Ki67^{+}$ MuSCs[26] significantly rose in TA and gastrocnemius of glycine-induced *mdx* mice compared to the saline control (Figures 3C and 3D), demonstrating that glycine promotes MuSC proliferation. Significantly higher amounts of FITC-labeled PMO were consistently found in increased numbers of eMyHC-positive regenerating fiber in TA and gastrocnemius of glycine-induced *mdx* mice than the saline control (Figures 3E and 3F), although no co-localization of FITC-labeled PMOs with MuSCs was found in gastrocnemius of glycine-induced or saline control mice (Figure S3D). Evident exon 23 skipping was consistently observed in TA and gastrocnemius from glycine-induced *mdx* mice compared to the saline-treated and untreated *mdx* controls (Figure 3G). Notably, glycine injection into TA muscles followed by PMO 3 days after significantly increased the number of dystrophin-positive fibers and levels of dystrophin expression (Figures S4A and S4B). Correspondingly, glycine could also be shown to enhance PMO uptake in differentiating myotubes in culture but not in proliferating myoblasts (Figure 3H). The results support the notion that glycine promotes muscle regeneration, which in turn results in

Figure 2. Long-Term Repeated Administrations of PMO in Glycine (PMO-G) or in Saline (PMO-S) in Adult *mdx* Mice

PMO-G was administered intravenously into adult *mdx* mice at 25 mg/kg/week for 3 weeks with additional glycine administration every other day intravenously followed by 25 mg/kg/month for 5 months with additional glycine administration every week intravenously. (A) Diagram of dosing regimen for the long-term study in *mdx* mice. i.v., intravenous injection. (B) Immunohistochemistry for dystrophin expression in body-wide muscles from *mdx* mice treated with PMO-S or PMO-G (scale bar, 100 μm). (C) Western blot for dystrophin expression in body-wide muscles from *mdx* mice treated with PMO-G or PMO-S. 2.5, 5, 10, and 25 μg of total protein from *C57BL/6* mice and 50 μg from muscle samples from untreated and treated *mdx* mice were loaded. TA, tibialis anterior; Q, quadriceps; G, gastrocnemius; T, triceps; A, abdominal muscle; D, diaphragm. (D) Quantitative analysis of dystrophin expression in body-wide muscles from treated *mdx* mice (n = 4; two-tailed t test). (E) Re-localization of DAPC components in treated *mdx* mice to assess dystrophin function and recovery of normal myoarchitecture (scale bar, 50 μm). The arrowheads point to identical myofibers. (F) Measurement of serum creatine kinase (CK) levels in treated *mdx* mice (n = 4; one-way ANOVA and *post hoc* Student-Newman-Keuls test). (G) Muscle function was assessed to determine the physical improvement with grip strength test (n = 4; one-way ANOVA and *post hoc* Student-Newman-Keuls test). (H) Measurement of muscle endurance with the running wheel test (n = 4; one-way ANOVA and *post hoc* Student-Newman-Keuls test). Data are presented as means ± SEM. *$p < 0.05$, **$p < 0.001$.

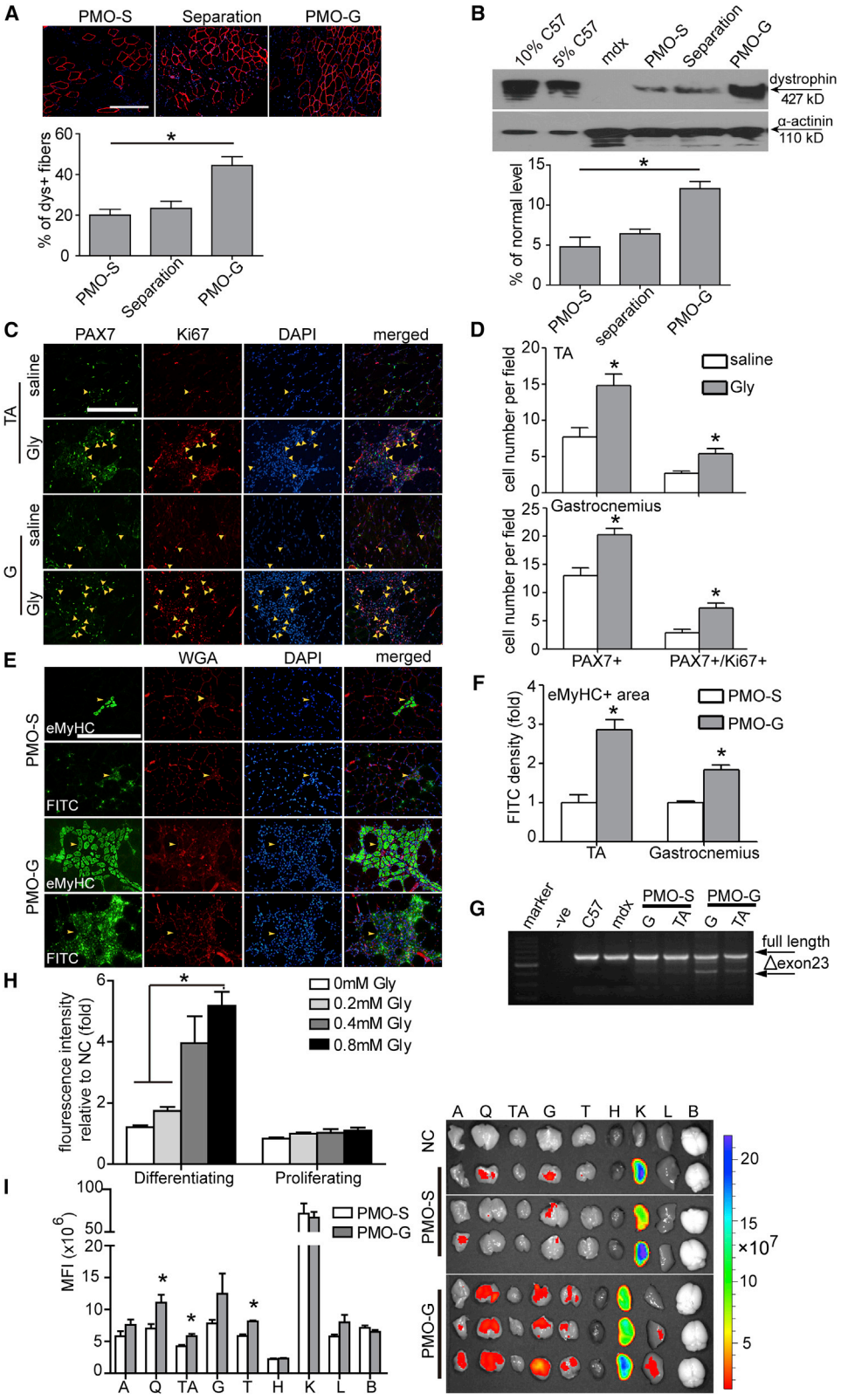

(legend on next page)

enhanced PMO uptake. Based on the observation, we adopted the glycine induction regimen and repeated the tissue distribution experiment with FITC-labeled PMO. As expected, significantly higher fluorescence was detected in peripheral muscles from glycine-induced *mdx* mice compared to the saline-treated and untreated *mdx* controls 48 h after injection (Figure 3I). These data strengthen the conclusion that glycine synergizes PMO therapy by promoting muscle regeneration, which in turn results in greater PMO uptake and efficacy.

Glycine Increases Muscle Regeneration by Replenishing the One-Carbon Unit Pool

To understand how glycine promotes muscle regeneration and whether active transport of glycine is critical for its functionality, we blocked glycine transporter 1 (GlyT-1), the ubiquitous glycine transporter,[27] with bitopertin (BP), an inhibitor for GlyT-1.[28] Strikingly, muscle regeneration was completely compromised in the presence of BP, as $PAX7^+$ or $PAX7^+/Ki67^+$ MuSCs (Figures 4A and 4B) and eMyHC-positive regenerating myofibers (Figure 4C) significantly declined in TA muscles co-administered with glycine and BP. PMO activities were consistently negated when BP was co-administered with PMO-G, as dystrophin-positive fibers (Figure 4D) and dystrophin expression (Figure 4E) significantly decreased, suggesting that active transport is vital for the functionality of glycine. As intracellular glycine is primarily metabolized as a one-carbon unit donor,[29] we examined whether glycine promotes muscle regeneration by providing one-carbon units, which are building blocks for nucleic acid and protein biosynthesis required for active MuSC proliferation.[30] Blockade of dihydrofolate reductase, a key enzyme required for reducing dihydrofolic acid to tetrahydrofolic acid for one-carbon transfer,[31] with methotrexate (MTX), an inhibitor of dihydrofolate reductase,[32] completely abolished glycine-induced effects on muscle regeneration, as $PAX7^+$ or $PAX7^+/Ki67^+$ MuSCs (Figures 4F and 4G) and eMyHC-positive regenerating myofibers (Figure 4H) significantly declined. To further validate this, we replaced glycine with formate, the only non-tetrahydrofolate (THF)-linked intermediate in one-carbon metabolism,[33] or THF, an intermediate carrier for one-carbon unit.[34] $PAX7^+$ or $PAX7^+/Ki67^+$ MuSCs (Figures 4F and 4G) and eMyHC-positive regenerating fibers (Figure 4H) significantly rose in formate- or THF-treated TA muscles compared to the saline control, suggesting that other one-carbon group donors or carriers can also enhance muscle regeneration, although to a lesser extent than glycine. If glycine functions as a one-carbon donor, a synergistic effect would be expected when glycine and THF were co-administered into TA muscles of *mdx* mice. A dramatic enhancement on MuSC proliferation (Figures 4F and 4G) and muscle regeneration (Figure 4H) was observed in TA muscles of *mdx* mice co-administered with glycine and THF compared to glycine alone. A positive correlation between muscle regeneration and PMO activities was concordantly established, as dystrophin-positive fibers (Figure 4I) and dystrophin expression (Figure 4J) significantly increased in TA muscles of *mdx* mice treated with PMO in formate, THF, or the combination of glycine and THF, whereas a significant decline was observed in *mdx* mice treated with glycine and MTX. However, glycine-induced muscle regeneration was significantly compromised when glycine decarboxylase (GLDC) P-protein, the key enzyme for glycine decarboxylation in the glycine cleavage system,[35] was down-regulated with GLDC-targeted short hairpin RNA (shRNA) delivered with AAV2/8 (Figure 5A), as $PAX7^+$ or $PAX7^+/Ki67^+$ MuSCs (Figures 5B and 5C) and eMyHC-positive regenerating fibers (Figure 5D) were significantly reduced in TA muscles from treated *mdx* mice. In parallel with reduced MuSC proliferation and muscle regeneration, dystrophin-positive fibers (Figure 5E) and dystrophin expression (Figure 5F) significantly decreased. These results support the conclusion that glycine contributes to MuSC proliferation and muscle regeneration by supplying one-carbon units.

Glycine Strengthens mTORC1 Activation and Contributes to Muscle Regeneration

It is known that mTORC1 is activated in muscle regeneration in response to injury,[36] and thus to investigate whether mTORC1 is involved in the muscle regeneration process of *mdx* mice, we measured levels of phosphorylated mTOR (p-mTOR) in *mdx* mice. Upregulation of p-mTOR was observed in TA muscles of *mdx* mice compared to age-matched wild-type *C57BL/6* controls (Figure S5A). Strikingly, levels of

Figure 3. Glycine Promotes PMO Uptake in Synergizing with Muscle Regeneration in *mdx* Mice

(A) Immunohistochemistry and quantitative analysis for dystrophin-positive fibers in *mdx* TA muscles injected with 2 μg of PMO followed by separate administration of glycine 16 h later (scale bar, 100 μm) (n = 3; one-way ANOVA and *post hoc* Student-Newman-Keuls test). Red staining on fiber membrane shows dystrophin expression. Nuclei were counterstained with DAPI (blue) (the same is true for the rest unless otherwise specified). (B) Western blot and quantitative analysis for the dystrophin protein in treated *mdx* mice (n = 3; one-way ANOVA and *post hoc* Student-Newman-Keuls test). (C) Immunohistochemistry for $PAX7^+$ and $Ki67^+$ muscle satellite cells (MuSCs) in TA and gastrocnemius muscles from *mdx* mice treated with saline or glycine every other day for 1 week intravenously (scale bar, 100 μm). TA, tibialis anterior. The arrowheads point to $PAX7^+$ and $Ki67^+$ MuSCs. (D) Quantitative analysis for $PAX7^+$ and $PAX7^+/Ki67^+$ MuSCs in TA and gastrocnemius muscles from treated *mdx* mice (n = 4; two-tailed t test). (E) Immunohistochemistry for embryonic myosin heavy chain -positive ($eMyHC^+$) regenerating myofibers in gastrocnemius from treated *mdx* mice. FITC-labeled PMO in glycine (PMO-G) or saline (PMO-S) was intravenously administered into adult *mdx* mice at 50 mg/kg for single injection and muscles were harvested 48 h later (scale bar, 100 μm). Fluorescently tagged wheat germ agglutinin (WGA) was used for the visualization of connective tissues. The arrowheads point to the $eMyHC^+$ regenerating myofibers and FITC-labeled PMO. (F) Quantitative analysis for the fluorescence intensity of $eMyHC^+$ regenerating myofibers in TA and gastrocnemius muscles from treated *mdx* mice (n = 3; two-tailed t test). (G) Representative RT-PCR to detect the exon-skipping efficiency, which is shown by shorter exon-skipped bands (indicated by Δexon 23, exon 23 skipped). G, gastrocnemius. (H) Measurement of the uptake of FITC-labeled PMO in differentiating and proliferating myoblasts treated with different concentrations of glycine (n = 4; one-way ANOVA and *post hoc* Student-Newman-Keuls test). NC refers to untreated differentiating myotubes or proliferating myoblasts. (I) Tissue distribution of FITC-labeled PMOs in *mdx* mice and quantitative analysis of fluorescence intensity in body-wide tissues. Body-wide tissues were harvested 48 h after single intravenous injection of FITC-labeled PMO in glycine (PMO-G) or saline (PMO-S) at the 50 mg/kg doses (n = 3; two-tailed t test). A, abdominal muscle; Q, quadriceps; TA, tibialis anterior; G, gastrocnemius; T, triceps; H, heart; K, kidney; L, liver; B, brain. Data are presented as means ± SEM. *$p < 0.05$.

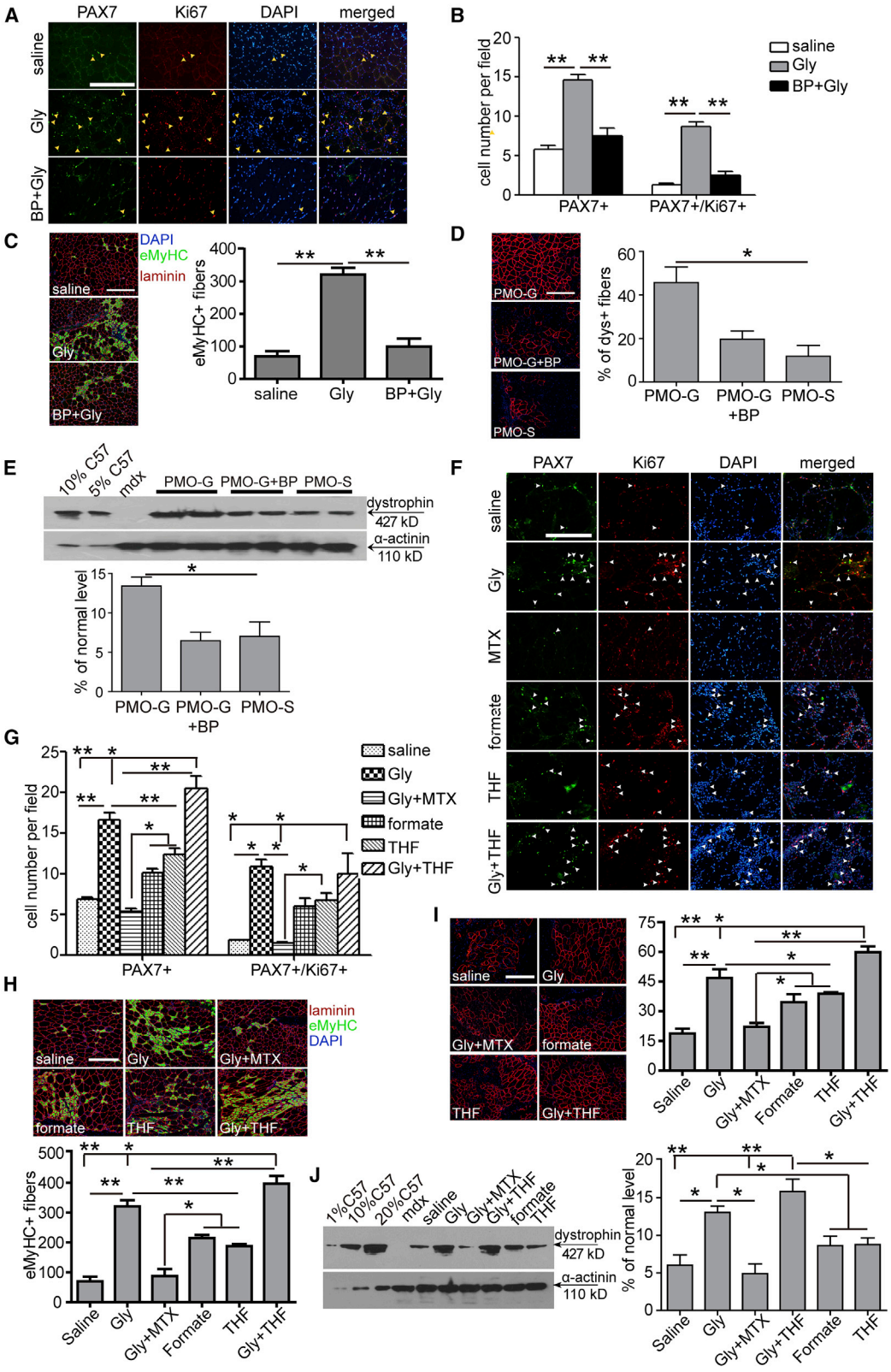

(legend on next page)

p-mTOR, phosphorylated ribosomal protein S6 kinase 1 (p-S6K1), a hallmark of specific activation by mTORC1, and phosphorylated ribosomal protein S6 (p-S6), a key downstream target of S6K1,[37] were elevated in quadriceps of *mdx* mice treated with PMO-G at 25 mg/kg/week for 3 weeks with additional glycine infusion compared to the saline control (Figures 6A and 6B). In contrast, there was no increase of p-mTOR and p-S6K1 in THF- or formate-treated TA muscles compared to glycine (Figures S5B and S5C), highlighting the glycine-specific hyperactivation of mTORC1. Blockade of mTORC1 activation with PP242 (Figures S5D and S5E), a small-molecule protein kinase inhibitor targeting the ATP-binding site of mTOR,[38] abolished the enhancement potentiated by glycine, as $PAX7^+$ or $PAX7^+/Ki67^+$ MuSCs (Figures 6C and 6D) and eMyHC-positive regenerating myofibers (Figure 6E) significantly declined. PMO activity was also negated as dystrophin-positive fibers (Figure 6F) and dystrophin expression significantly decreased (Figure 6G) in TA muscles from treated *mdx* mice, confirming the relevance of mTORC1 in the functionality of glycine. Analysis of the gene expression profiles of glycine-treated primary myoblasts, isolated from adult *mdx* mice, revealed that glycine significantly upregulated two annotated groups of genes, that is, cell cycle and metabolism (Figures 6H and S5F), with upregulation of cyclin-dependent kinase 1 (*CDK1*), cell division cycle 20 (*CDC20*), and cyclin B2 (*CCNB2*) genes validated by quantitative real-time reverse transcriptase (RT)-PCR (Figure 6I), demonstrating that glycine promotes cell proliferation. These results demonstrate that glycine strengthens mTORC1 activation, which in turn promotes MuSC proliferation and muscle regeneration.

Glycine Triggers mTORC1 via v-ATPase

To elucidate how glycine regulates mTORC1, we used murine myoblasts (C2C12), which were shown to be responsive to glycine,[39,40] and human embryonic kidney 293T (HEK293T) cells, a commonly used cellular model.[41] To verify whether C2C12 and HEK293T cells are responsive to glycine stimulation, we examined cell growth in the absence or presence of glycine *in vitro*. Deprivation of total amino acids significantly inhibited C2C12 and HEK293T cell growth, whereas the supplementation of glycine or total amino acids 24 h after starvation stimulated cell growth in glycine- or total amino acid-depleted cells (Figure S6A), indicating that C2C12 and HEK293T cells respond to glycine. Levels of p-S6K1 and phosphorylated eukaryotic initiation factor 4E-binding protein 1 (p-4E-BP1), the two best characterized downstream targets of mTORC1 and a readout for mTORC1 activity,[42] and the downstream target p-S6 were concordantly elevated in glycine- or total amino acid-supplemented C2C12 cells compared to total amino acid-depleted cells (Figures 7A and 7B). As amino acids were shown to transfer signals to mTOR by promoting its translocation to the surface of lysosomes where mTORC1 is activated,[43] we starved C2C12 cells for 60 min and re-stimulated them with glycine or total amino acids for 20 min. Localization of mTOR in conditions of amino acid starvation was predominantly cytoplasmic and presented a diffuse staining pattern, with little co-localization being observed with lysosome-associated membrane protein 1 (LAMP1), a lysosomal marker,[44] whereas glycine or total amino acid stimulation led to mTOR clustered with lysosomes (Figures 7C and 7D). A similar pattern was observed in total amino acid-starved HEK293T cells followed by glycine or total amino acid supplementation (Figures S6B and S6E). These results proved that glycine can promote recruitment of mTOR to the lysosome. To substantiate the notion that glycine enables the translocation of mTOR to the lysosome, we blocked the vacuolar H^+-adenosine triphosphatase ATPase (v-ATPase), a component necessary for amino acids to activate mTORC1,[43] with bafilomycin A1 (BAF),[45] a highly specific inhibitor of the V-ATPase. Glycine-induced mTORC1 activation was substantially blocked with BAF in HEK293T cells, as co-localization of mTOR with lysosomes (Figures 7E and 7F) and levels of p-S6K1 and p-S6 (Figure 7G) were significantly reduced compared to glycine. As the Ras-related GTPase (Rag) is known to mediate the amino acid signal to mTOR and facilitate the binding of mTOR to lysosomes,[46] we disrupted RagB expression in HEK293T cells with the CRISPR-Cas9 system. Phosphorylation of S6K1 and S6 was completely abolished in total amino acid-depleted RagB knockout cells after stimulation with glycine or total amino acids for 10, 20, or 30 min (Figure 7H), demonstrating that RagB is responsible for the recruitment of mTOR to the surface of lysosomes.

Figure 4. Glycine Potentiates PMO Activity by Replenishing One-Carbon Unit Pool

(A) Immunohistochemistry for $PAX7^+$ and $Ki67^+$ MuSCs in TA muscles from *mdx* mice treated with PMO-G and bitopertin (BP) (scale bar, 100 μm). Glycine or the mixture of glycine and BP was administered into *mdx* TA muscles and muscles were harvested 3 days later. The arrowheads point to $PAX7^+$ and $Ki67^+$ MuSCs. (B) Quantitative analysis for $PAX7^+$ and $PAX7^+/Ki67^+$ MuSCs in TA muscles from treated *mdx* mice (n = 3; one-way ANOVA and *post hoc* Student-Newman-Keuls test). (C) Immunohistochemistry and quantitative analysis for $eMyHC^+$ regenerating myofibers in TA muscles from treated *mdx* mice (scale bar, 100 μm) (n = 3; one-way ANOVA and *post hoc* Student-Newman-Keuls test). (D) Immunohistochemistry and quantitative analysis for dystrophin-positive fibers in TA muscles from treated *mdx* mice (scale bar, 100 μm) (n = 3; one-way ANOVA and *post hoc* Student-Newman-Keuls test). PMO (2 μg) in saline and other solutions was injected into *mdx* TA muscles and muscles were harvested 2 weeks later. (E) Western blot and quantitative analysis for dystrophin expression in TA muscles from treated *mdx* mice (n = 3; one-way ANOVA and *post hoc* Student-Newman-Keuls test). 2.5 and 5 μg of total protein from *C57BL/6* mice and 50 μg from muscle samples from untreated and treated *mdx* mice were loaded. (F) Immunohistochemistry for $PAX7^+$ and $Ki67^+$ MuSCs in TA muscles from treated *mdx* mice (scale bar, 100 μm). Glycine, formate, tetrahydrofolate (THF), or the mixture of glycine with methotrexate (MTX) or THF was injected in *mdx* TA muscles and muscles were harvested 3 days later. The arrowheads point to $PAX7^+$ and $Ki67^+$ MuSCs. (G) Quantitative analysis for $PAX7^+$ and $PAX7^+/Ki67^+$ MuSCs in TA muscles from treated *mdx* mice (n = 3; one-way ANOVA and *post hoc* Student-Newman-Keuls test). (H) Immunohistochemistry and quantitative analysis for $eMyHC^+$ regenerating myofibers in TA muscles from treated *mdx* mice (scale bar, 100 μm) (n = 3; one-way ANOVA and *post hoc* Student-Newman-Keuls test). (I) Immunohistochemistry and quantitative analysis for dystrophin-positive fibers in TA muscles from treated *mdx* mice (scale bar, 100 μm) (n = 3; one-way ANOVA and *post hoc* Student-Newman-Keuls test). (J) Western blot and quantitative analysis for dystrophin expression in TA muscles from treated *mdx* mice (n = 3; one-way ANOVA and *post hoc* Student-Newman-Keuls test). 0.5, 5, and 10 μg of total protein from *C57BL/6* mice and 50 μg from muscle samples from untreated and treated *mdx* mice were loaded. Data are presented as means ± SEM. *$p < 0.05$, **$p < 0.001$.

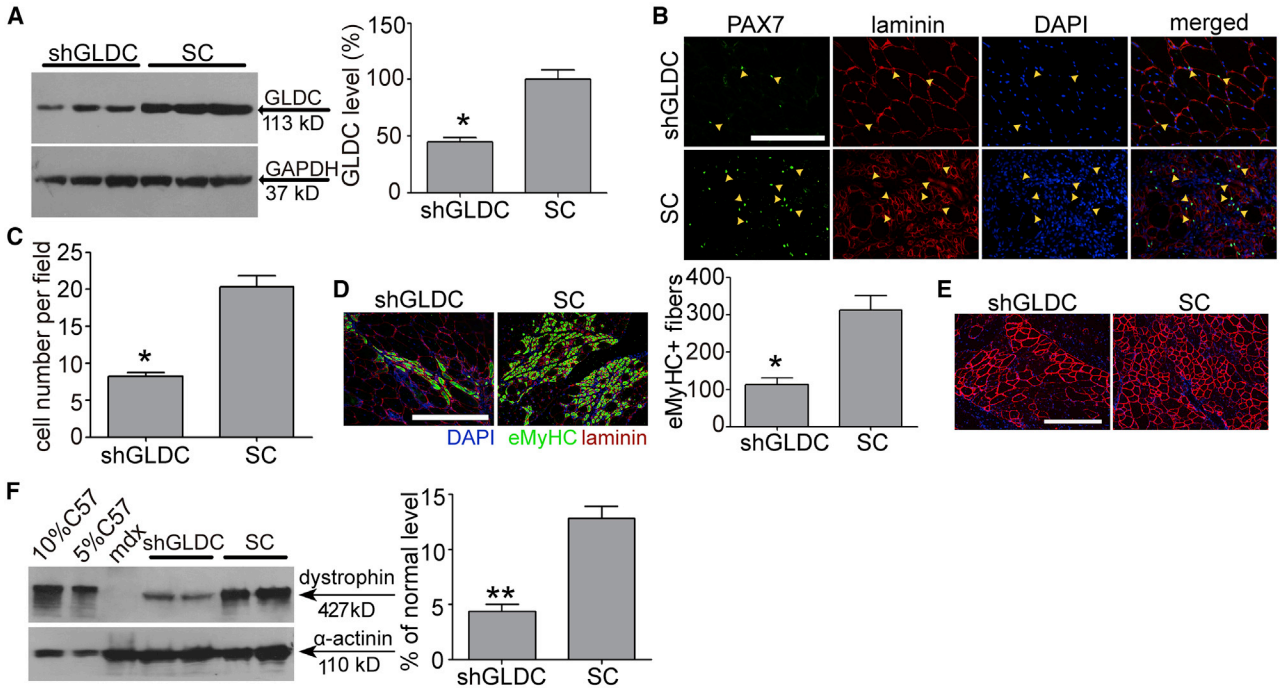

Figure 5. Disruption of Glycine Decarboxylase (GLDC) Compromises the Functionality of Glycine in *mdx* Mice

(A) Western blot analysis to determine *GLDC* knockdown efficiency at the protein level in TA muscles transfected with *GLDC* shRNA-expressing AAV2/8 viruses in *mdx* mice 3 weeks later (n = 3). SC refers to AAV2/8 expressing scramble shRNA. (B) Immunohistochemistry for PAX7$^+$ MuSCs in TA muscles from treated *mdx* mice (scale bar, 100 μm). The arrowheads point to PAX7$^+$ MuSCs. (C) Quantitative analysis for PAX7$^+$ MuSCs in TA muscles from treated *mdx* mice (n = 3). (D) Immunohistochemistry and quantitative analysis for eMyHC$^+$ regenerating myofibers in TA muscles from treated *mdx* mice (n = 3) (scale bar, 100μm). (E) Immunohistochemistry for dystrophin-positive fibers in TA muscles from treated *mdx* mice (scale bar, 100 μm). (F) Western blot and quantitative analysis for dystrophin expression in TA muscles from treated *mdx* mice (n = 4). 2.5 and 5 μg of total protein from *C57BL/6* mice and 50 μg of muscle samples from untreated and treated *mdx* mice were loaded. Two-tailed t test was used for statistical analysis. *$p < 0.05$, **$p < 0.001$. Data are presented as means ± SEM.

Glycine Enhances Cell Transplantation in *mdx* Mice

Given the dramatic effect of glycine on endogenous MuSC proliferation, we examined whether glycine has any benefit on exogenous cell transplantation. To this end, we adopted the commonly used cardiotoxin (CTX) injury model by injecting CTX to TA muscles of *mdx* mice 1 day prior to transplantation.[47] Pre-administration of glycine was shown to suppress immunological reactions in liver transplantation,[16,48] and therefore we intravenously administered glycine into *mdx* mice 7 days prior to transplantation and supplied glycine during the experimental period as illustrated in Figure 8A. MuSCs (1×10^5) derived from wild-type *C57BL/6* mice were transplanted into CTX-injured TA muscles of immunosuppressed adult *mdx* mice (Figure 8A). Dystrophin-positive fibers (Figure 8B) and muscle weight (Figure 8C) were significantly increased in TA muscles 3 weeks after cell transplantation in the glycine group compared to the saline control. Increased cell transplantation efficiency was consistently observed when wild-type *C57BL/6* primary myoblasts (1×10^6) were transplanted into TA muscles of glycine-induced *mdx* mice under identical conditions (Figure 8D). In line with the previous observation,[39] glycine promoted murine primary myoblast proliferation (Figure S7). To further confirm the beneficial effect of glycine on cell transplantation, we transplanted EGFP-positive PAX7$^+$MyoD$^+$ MuSCs derived from transgenic *C57BL/6* EGFP mice (Figure S8A) into CTX-injured TA muscles of glycine-induced *mdx* mice and monitored the fluorescence in a real-time manner. Stronger fluorescence was detected in TA muscles from glycine-induced *mdx* mice than from the saline control at different time points after transplantation with live animal imaging (Figure S8B). Significantly stronger fluorescence signals were consistently detected in TA muscles isolated from glycine-induced *mdx* mice compared to the saline control at week 3 after transplantation (Figure 8E). Co-localization of EGFP-positive fibers with significantly increased numbers of dystrophin-positive fibers (Figures 8F and 8G) confirmed the benefits of glycine on exogenous MuSC transplantation. These findings support the conclusion that glycine enhances cell transplantation.

DISCUSSION

Glycine is known to have a wide spectrum of functions against different injuries and diseases.[16] In this study, we demonstrate that glycine promotes the potency of PMOs and cell transplantation in dystrophic mice. Therapeutic levels of dystrophin and functional improvement were achieved in *mdx* mice with extremely low doses of PMO (25 mg/kg) without any detectable toxicity. Importantly,

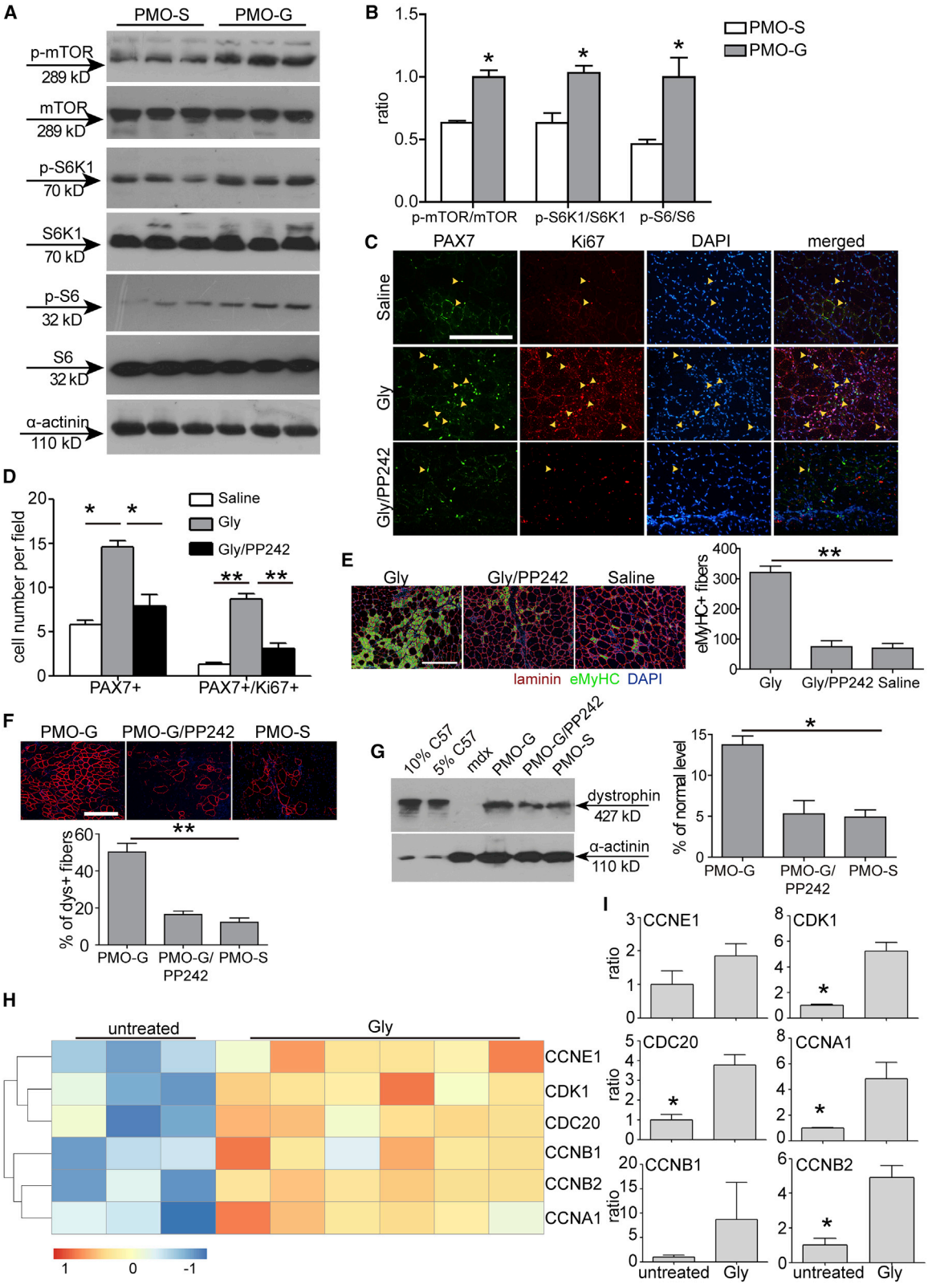

(legend on next page)

up to a 50-fold higher level of dystrophin was produced in abdominal muscles of PMO-G-treated *mdx* mice compared to PMO-S, showing the potency of glycine in improving this low dose of PMO. Dissection of glycine functionality revealed that glycine promotes muscle regeneration, which in turn results in increased PMO uptake and consequent dystrophin expression in muscle. Mechanistically, glycine potentiates muscle regeneration by strengthening mTORC1 activation via RagB and v-ATPase and replenishing the one-carbon unit pool. Strikingly, glycine improves not only endogenous MuSC proliferation but also exogenous cell transplantation efficiency in dystrophic mice. Our study provides a simple approach for improving the efficacy of nucleic acid therapeutics and cell therapy and also insight for the role of glycine.

Glycine is vital for mammalian metabolism and nutrition and is considered a conditionally essential amino acid, and therefore it has been extensively used as a food additive.[49] In our current study, we further confirmed its safety and biocompatibility, as repeated administrations of a physiological concentration of glycine (120 μL of 50 mg/mL into adult *mdx* mice, which would have a total blood volume of 1.46 mL) with PMO elicited significant functional rescue without any detectable toxicity. Although therapeutic levels of dystrophin were restored in body-wide peripheral muscles with low doses of PMO when administered with glycine, we failed to detect any dystrophin expression in the heart, and dystrophin typically becomes detectable in dystrophic hearts only when the dose of PMO is 300 mg/kg.[50] Interestingly, marginal improvements in cardiac functions were observed in the heart from repeated treatments of PMO-G for 6 months compared to PMO-S and untreated age-matched *mdx* controls (data not shown). Further studies with peptide-modified PMOs[51] are warranted to determine whether heart delivery can be achieved, as the heart is particularly challenging to deliver to.

Interestingly, unlike hexose,[19] glycine promotes PMO uptake by activating MuSC proliferation and muscle regeneration rather than directly improving PMO uptake in dystrophic muscles. Thus, it might be unnecessary to administer glycine together with PMO for future clinical uses. Glycine can be taken via dietary supplementation, whereas PMO drugs can be administered via the delivery route approved by FDA, which can enhance the therapeutic efficacy of approved DMD AO drugs without the requirement for further clinical assessment. Glycine not only provides necessary nutrition for DMD patients and promotes satellite cell proliferation, but it also serves as an enhancer for approved AO drugs and eases DMD patients' economic burdens by reducing the dose and related costs; therefore, glycine may kill four birds with one stone. Notably, a significant body weight gain was observed in PMO-G-treated *mdx* mice compared to PMO-S in the long-term study, which is likely attributed to the increased muscle mass stimulated with glycine in combination with dystrophin restoration, as no body weight gain was observed in *mdx* mice with glycine alone (unpublished data). In addition, we investigated the effect of PMO-G in aged *mdx* mice, which showed more severe inflammation and fibrosis with much less muscle preserved,[52] and a similar potency was achieved with enhanced muscle regeneration and PMO activities (data not shown), further highlighting the benefits of glycine in treating DMD patients irrespective of ages. Also note that recent studies with glycine alone or glycine together with prednisolone extended lifespan of mice or alleviated the pathological progression in dystrophic mice,[53,54] further confirming the beneficial effect of glycine in general.

Another important finding from our current study is that we demonstrated that glycine can activate mTORC1, a central nutrient-sensing pathway,[55] in dystrophic muscle. Amino acids are shown to communicate with mTORC1 via a lysosome-based signaling system; however, it remains unclear about how amino acids regulate mTORC1, as the existence of different transport mechanisms for amino acids complicates the situation.[56] In our study, although we proved that glycine-specific mTORC1 activation was involved in muscle regeneration in dystrophic mice and glycine likely activates mTORC1 via v-ATPase and RagB, two key components for the shuttle of mTORC1 from peripheral to lysosomes,[46] further studies are warranted to address how mTORC1 senses glycine in muscle.

One major hurdle for the clinical implementation of cell therapy is the low transplantation efficiency, which is likely due to poor retention

Figure 6. Glycine Augments PMO Activities by Heightening mTORC1 Activation in *mdx* Mice

(A) Western blot to detect phosphorylated mTOR, S6K1, and S6 expression in quadriceps from *mdx* mice treated intravenously with PMO-S or PMO-G at 25 mg/kg/week for 3 weeks with additional supply of glycine every other day for 5 weeks. α-Actinin was used as the loading control. 50 μg of total protein was loaded. (B) Quantitative analysis of the ratio of phosphorylated mTOR, S6K1, and S6 to mTOR, S6K1, and S6 total protein expression, respectively (n = 3; two-tailed t test). (C) Immunohistochemistry for $PAX7^+$ and $Ki67^+$ MuSCs in TA muscles from treated *mdx* mice (scale bar, 100 μm). Glycine (Gly) or the mixture of glycine with PP242 (Gly/PP242) was injected into *mdx* TA muscles and muscles were harvested 3 days later. The arrowheads point to $PAX7^+$ and $Ki67^+$ MuSCs. (D) Quantitative analysis for $PAX7^+$ and $PAX7^+/Ki67^+$ MuSCs in TA muscles from treated *mdx* mice (n = 3; one-way ANOVA and *post hoc* Student-Newman-Keuls test). (E) Immunohistochemistry and quantitative analysis for $eMyHC^+$ regenerating myofibers in TA muscles from treated *mdx* mice (n = 3; one-way ANOVA and *post hoc* Student-Newman-Keuls test) (scale bar, 100μm). (F) Immunohistochemistry and quantitative analysis for dystrophin-positive fibers in TA muscles from treated *mdx* mice (scale bar, 100 μm) (n = 3; one-way ANOVA and *post hoc* Student-Newman-Keuls test). PMO (2 μg) in saline (PMO-S), glycine (PMO-G), or the mixture of glycine with PP242 (PMO-G/PP242) was injected into *mdx* TA muscles and muscles were harvested 2 weeks later. (G) Western blot and quantitative analysis for dystrophin expression in TA muscles from treated *mdx* mice (n = 3; one-way ANOVA and *post hoc* Student-Newman-Keuls test). 2.5 and 5 μg of total protein from *C57BL/6* mice and 50 μg of muscle samples from untreated and treated *mdx* mice were loaded. (H) Hierarchical clustering analysis of cell cycle-related gene expression profiles in primary myoblasts isolated from *mdx* mice and then treated with 0.8 mM glycine for 24 h. Expression levels (fold) are depicted in colors in which red represents upregulation and green means downregulation. (I) Quantitative real-time RT-PCR analysis of cell cycle-related gene expression in TA muscles from *mdx* mice treated with glycine every other day for 1 week intravenously (n = 3; two-tailed t test). CDK1, cyclin-dependent kinase 1; CDC20, cell division cycle 20; CCNB2, cyclin B2; CCNB1, cyclin B1; CCNA1, cyclin A1; CCNE1, cyclin E1. Data are presented as means ± SEM. *$p < 0.05$, **$p < 0.001$.

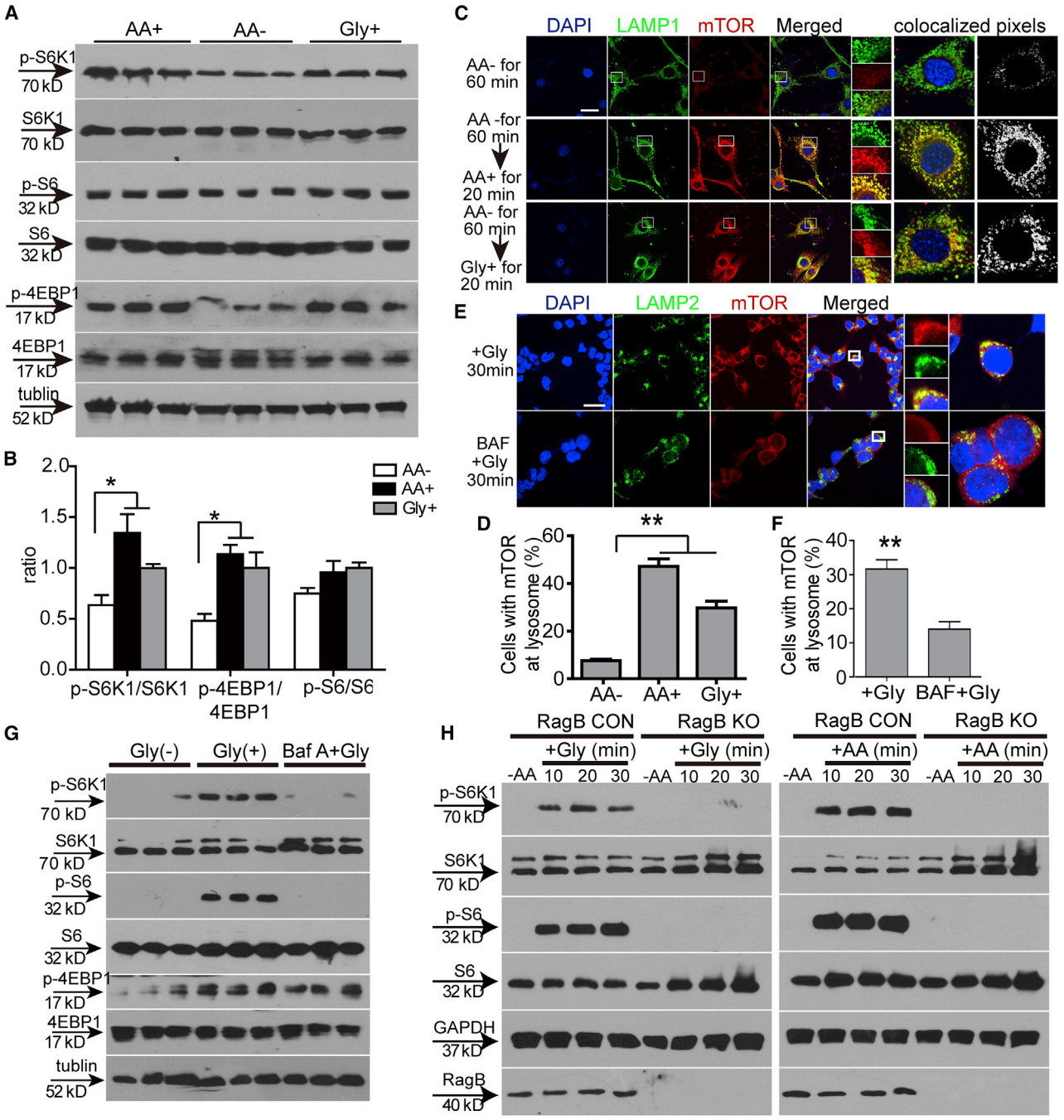

Figure 7. Glycine Promotes mTORC1 Translocation via v-ATPase and RagB

(A) Western blot to detect phosphorylated S6K1, S6, and 4EBP1 expression in starved C2C12 cells followed by re-stimulation of total amino acids and glycine. 30 μg of total protein was loaded and tubulin was used as a loading control. AA^+ refers to the supplementation of total amino acids; Gly^+ refers to the supplementation of glycine into starved cells; AA^- represents the depletion of total amino acids. (B) Quantitative analysis of the ratio of phosphorylated S6K1, S6, and 4EBP1 to total expression of counterparts (n = 3; one-way ANOVA and *post hoc* Student-Newman-Keuls test). (C and D) Immunocytochemistry for mTOR (C) and quantitative analysis of cells with mTOR at lysosomes (D) in starved C2C12 cells followed by re-stimulation of total amino acids or glycine (scale bar, 10 μm) (n = 10; one-way ANOVA and *post hoc* Student-Newman-Keuls test). LAMP1 and LAMP2 were used as lysosome markers. (E and F) Immunocytochemistry for mTOR (E) and quantitative analysis of cells with mTOR at lysosomes (F) in HEK293T cells treated with glycine and BAF (scale bar, 10 μm) (n = 10; two-tailed t test). (G) Western blot to detect phosphorylated S6K1 and S6 expression in HEK293T

(legend continued on next page)

and survival of transplanted cells.[57] In this study, we show that glycine not only promotes endogenous MuSC proliferation but also increases exogenous cell transplantation efficiency in dystrophic mice, suggesting that glycine can improve cell therapy. We adopted the protocol of pre-administration based on the assumption that glycine can prevent the activation of immune cells, as shown for liver transplantation,[16] and we monitored the fluorescence of EGFP-positive MuSCs after transplantation in CTX-injured TA muscles of *mdx* mice in a real-time manner. Although the results showed stronger fluorescence signals in TA muscles from glycine-induced mice compared to the saline control at different time points after transplantation, we were uncertain about whether the presence of glycine increases cell retention and survival or promotes its proliferation due to the low fluorescence intensity and auto-fluorescence from muscle. Further detailed studies to understand how glycine impacts cell transplantation are warranted. Nevertheless, our study demonstrated a proof of concept that glycine can enhance cell transplantation.

In summary, we demonstrate that glycine potentiates AO efficacy and cell transplantation and thus opens a fundamentally new avenue to overcome the challenge of *in vivo* systemic delivery of nucleic acids and cell therapy. Moreover, our findings unveil the role of glycine as an activator of the mTORC1 pathway in muscular dystrophies.

MATERIALS AND METHODS

Animals and Injections

Adult *mdx* mice (6–8 weeks old) and age-matched *C57BL/6* mice were used in all experiments (the number of mice per group is specified in corresponding figure legends). Mice were housed under specific pathogen-free conditions in a temperature-controlled room. The experiments were carried out in the Animal Unit, Tianjin Medical University (Tianjin, China), according to procedures authorized by the Institutional Ethics Committee (permit no. SYXK 2009-0001). For local intramuscular injection, 2 μg of PMO was dissolved in saline or other solutions. For intravenous injections, various amounts of PMO in 120 μL of saline or amino acid solutions was injected into the tail vein of *mdx* mice at 25 or 50 mg/kg per week for 3 weeks. For the long-term systemic study, PMO in glycine or saline was repeatedly injected at 25 mg/kg per week for 3 weeks with 50 mg/mL glycine administered every other day for the first 3 weeks, followed by 25 mg/kg per month for 5 months with 50 mg/mL glycine injected weekly in *mdx* mice intravenously. For mechanistic studies, 2 μg of PMO was dissolved in glycine with 0.2 μg of THF, 0.2 μg of MTX (Sigma, USA),[58] or 3 μg of BP or 5 μg of PP242 (Selleck Chemicals, USA),[59] or 2 μg of PMO was dissolved in 50 mg/mL formate (Sigma, USA) or 0.4 μg of THF.[58] Mice were killed by CO_2 inhalation at 2 weeks after the last injection unless otherwise specified, and muscles and other tissues were snap frozen in liquid nitrogen-cooled isopentane and stored at −80°C.

Oligonucleotides

Unlabeled and FITC- or lissamine-labeled PMO were synthesized by GeneTools (Corvallis, OR, USA). PMO (5′-GGCCAAACCTCGGC TTACCTGAAAT-3′) sequences were targeted to the murine *dmd* exon 23/intron 23 boundary site.[60]

Protein Extraction and Western Blot

For the detection of dystrophin in muscle tissues, western blot was performed as described previously.[19] Briefly, total protein was extracted from frozen muscles and the protein concentration was quantified by a Bradford assay (Sigma, USA). Various amounts of protein from wild-type *C57BL/6* mice were used as positive controls, and corresponding amounts of protein from muscles of treated or untreated *mdx* mice were loaded onto SDS-polyacrylamide electrophoresis gels (4% stacking and 6% resolving), followed by transfer to the polyvinylidene fluoride (PVDF) membrane. The membrane was then washed and blocked with 5% skimmed milk and probed overnight with primary mouse monoclonal antibodies, including DYS1 (1:200, Novo-Castra, UK) and α-actinin (1:4,000, Sigma-Aldrich, USA). For the detection of mTOR and other related proteins, 4% stacking and 6% resolving or 4% stacking and 10% resolving SDS-polyacrylamide electrophoresis gels were used, respectively. The following primary antibodies were used at the indicated dilution for western blot analysis: rabbit monoclonal antibodies, including mTOR (1:1,000), p-mTOR (1:500), S6 ribosomal protein (1:1,000), p-S6 ribosomal protein (1:1,000), p-4E-BP1 (1:500), RagB (1:1,000), p70S6K (1:500), p-p70S6K (1:500), GAPDH (1:1,000; Cell Signaling Technology, USA); 4E-BP1 (1:4,000, Abcam, UK); and α-tubulin mouse monoclonal antibody (1:1,000; Abcam, UK). Secondary horseradish peroxidase (HRP)-tagged antibody (1:4,000; Sigma, USA) was used and signals were visualized with an enhanced chemiluminescence (ECL) western blotting analysis system (Amersham Pharmacia Biosciences). Bands were quantified by densitometric analysis using ImageJ software program (NIH, USA). The dystrophin/α-actinin ratios of treated samples were normalized to the average *C57BL/6* dystrophin/α-actinin ratios (from serial dilutions). The ratio of phosphorylated mTOR and other proteins relative to corresponding total protein expression was calculated based on the mean value of band intensity with ImageJ software. At least three biological samples were examined unless otherwise specified.

Immunohistochemistry

Immunohistochemistry for dystrophin and eMyHC was performed as previously described.[19] Briefly, 8-μm cryosections were fixed in Dulbecco's PBS (DPBS) for 10 min and blocked for 1 h in DPBS supplemented with 20% goat serum and 10 mg/mL BSA (Sigma-Aldrich, MO, USA). Rabbit polyclonal antibody 2166 against the dystrophin C-terminal region (1:50; the antibody provided by Prof. Kay Davies, Department of Physiology, Anatomy and Genetics, University of Oxford), mouse monoclonal antibody BF-45 (1:30; Developmental

cells treated with glycine or glycine and BAF. 30 μg of total protein was loaded and tubulin was used as a loading control. (H) Western blot to detect phosphorylated S6K1 and S6 expression in RagB knockout HEK293T cells treated with glycine or total amino acids. 30 μg of total protein was loaded and GAPDH was used as a loading control. RagB CON refers to normal HEK293T cells; RagB KO means RagB knockout HEK293T cells. Data are presented as means ± SEM. *$p < 0.05$, **$p < 0.001$.

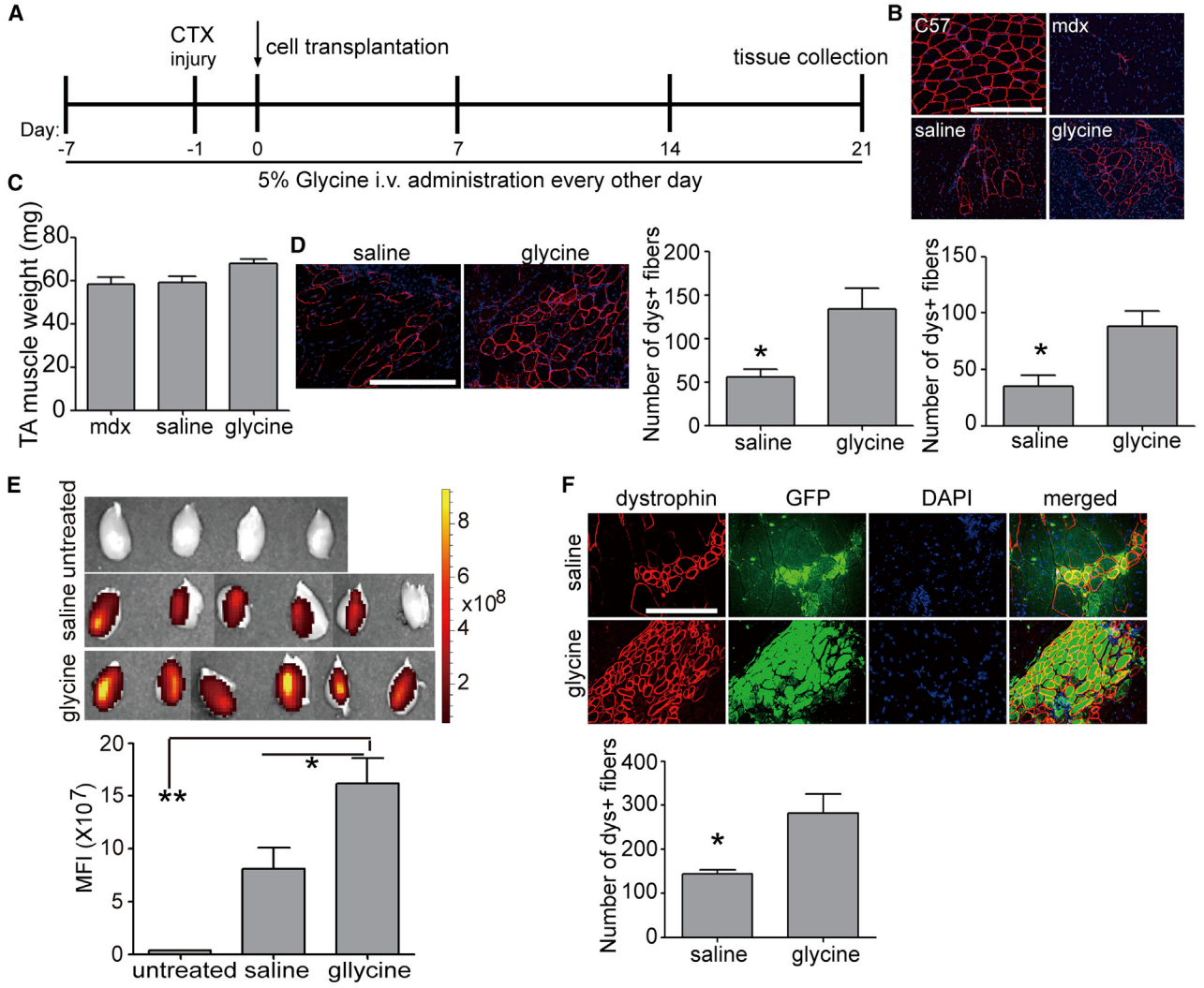

Figure 8. Effects of Glycine on Cell Transplantation in *mdx* Mice

(A) Schematics for the cell transplantation in immunosuppressed *mdx* mice. i.v., intravenous injection; −7, 7 days prior to cell transplantation; −1, 1 day prior to cell transplantation. *mdx* mice were immunosuppressed during the experimental period unless otherwise specified. (B) Immunohistochemistry and quantitative analysis for dystrophin-positive fibers in TA muscles from glycine-treated *mdx* mice transplanted with wild-type MuSCs and muscles were harvested 3 weeks later (scale bar, 100 μm) (n = 4; two-tailed t test). (C) Measurement of TA muscle weight from *mdx* mice transplanted with MuSCs 3 weeks after transplantation. *mdx* refers to *mdx* controls without cell transplantation (n = 4). (D) Immunohistochemistry and quantitative analysis for dystrophin-positive fibers in TA muscles from glycine-treated *mdx* mice transplanted with wild-type primary myoblasts 3 weeks after transplantation (scale bar, 100 μm) (n = 4; two-tailed t test). (E) Tissue imaging to examine the GFP fluorescence and quantitative analysis of fluorescence intensity in glycine-treated *mdx* mice transplanted with wild-type GFP-positive MuSCs 3 weeks after transplantation (scale bar, 100 μm) (n = 6; one-way ANOVA and *post hoc* Student-Newman-Keuls test). (F and G) Immunohistochemistry (F) and quantitative analysis for dystrophin- and GFP-positive fibers (G) in TA muscles from glycine-treated *mdx* mice transplanted with GFP-positive MuSCs 3 weeks later (scale bar, 100 μm) (n = 6; two-tailed t test). Data are presented as means ± SEM. *p < 0.05, **p < 0.001.

Studies Hybridoma Bank, University of Iowa, USA), and laminin (1:400; rabbit monoclonal antibody, Abcam, UK) were used. For the detection of DAPC components, serial sections were stained with a panel of polyclonal and monoclonal antibodies as described previously.[19] Briefly, rabbit polyclonal antibody to neuronal nitric oxide synthase (1:50) and mouse monoclonal antibodies to β-dystroglycan, α-sarcoglycan, and β-sarcoglycan were used according to the manufacturer's instructions (1:200, Novocastra, UK). Polyclonal antibodies were detected by goat anti-rabbit IgG-Alexa Fluor 594 and the monoclonal antibodies were detected by goat anti-mouse IgG-Alexa Fluor 594 (Molecular Probes, UK). The mouse-on-mouse (M.O.M.) blocking kit (Vector Laboratories, Burlingame, CA, USA) was applied for the immunostaining of the DAPC. For the immunostaining of PAX7, Ki67, and laminin,[61] 8-μm cryosections were fixed with 4% paraformaldehyde (PFA) for 15 min at room temperature (RT), followed by washing with 1% Triton X-100 in PBS for 5 min

three times. Subsequently, slides were immersed in pH 6.0 citrate buffer heated at 100°C for 10 min, followed by blocking with 10% AffiniPure Fab goat anti-mouse IgG (1:10; Jackson ImmunoResearch, USA) in 1% Triton X-100 for 1 h at RT and replaced with 20% goat serum and 10 mg/mL BSA in 1% Triton X-100 for 30 min at RT prior to incubation with PAX7 mouse monoclonal antibody (1:300; a gift from the Prof. Hongbo Zhang, ZhongShan University, GuangZhou, China) and Ki67 (1:1,000; rabbit monoclonal antibody, Abcam, UK). Rabbit monoclonal antibody was detected by goat anti-rabbit IgG-Alexa Fluor 594, and mouse monoclonal antibodies were detected by goat anti-mouse IgG-Alexa Fluor 488 (Invitrogen, USA). For the detection of FITC-labeled PMO in muscle tissues, 8-μm cryosections were fixed with 4% PFA for 15 min at RT, followed by fixation with ice-cold acetone for 10 min. Subsequently, sections were blocked in DPBS supplemented with 20% goat serum and 10 mg/mL BSA for 1 h, followed by incubation with anti-fluorescein (1:200, Life Technologies, MA, USA) overnight at 4°C. Wheat germ agglutinin-Alexa Fluor 647 (1:500; Life Technologies, MA, USA) was applied to the sections for 10 min at RT and washed with DPBS three time for 5 min each time. Sections were mounted with in fluorescent mounting medium (Dako, CA, USA) with 0.1% DAPI.

Cell Culture

HEK293T cells or murine C2C12 myoblasts were kept in-house and cultured at 37°C in 5% CO_2 in Dulbecco's modified Eagle's medium (DMEM) supplemented with 10% fetal bovine serum (FBS) and 1% penicillin and streptomycin. HEK293T cells (7×10^3) or murine C2C12 myoblasts (9×10^3) were seeded in 96-well plates for 12 h prior to the replacement with total amino acid-free high glucose DMEM (Thermo Fisher Scientific, USA) for 1 h, followed by the addition of total amino acid mixture consisting of MEM amino acids solution (1:50 v/v) and MEM non-essential amino acids solution (1:100 v/v) (Thermo Fisher Scientific, USA) or 0.8 mM glycine (Sigma, USA) for 24 h. Cells were counted with a hemocytometer. For the amino acid starvation experiments, 10% dialyzed FBS was depleted unless otherwise indicated.[46] For the v-ATPase blocking experiment, 1 μM BAF (MedChemExpress, USA) was added into the starved cells for 1 h prior to stimulation with total amino acids or glycine for 30 min. To examine the effect of different concentrations of glycine on PMO uptake in differentiating myotubes and proliferating myoblasts, FITC-labeled PMO (1 μM) and different concentrations of glycine were added into differentiating myotubes (24 h after differentiation induction) and proliferating myoblasts. The fluorescence was measured 48 h later with a plate reader.

Immunocytochemistry

HEK293T cells (1×10^4) or murine C2C12 myoblasts (1×10^4) were seeded on Matrigel-coated glass coverslips in 24-well plates for 24 h prior to the replacement with total amino acid-free high glucose DMEM (Thermo Fisher Scientific, USA) for 1 h, followed by the addition of total amino acid mixture consisting of MEM amino acids solution (1:50 v/v) and MEM non-essential amino acids solution (1:100 v/v) (Thermo Fisher Scientific, USA) or 0.8 mM glycine (Sigma, USA) for 10, 20, or 30 min. Cells were fixed with 4% PFA and permeabilized with 0.5% Triton X-100 in DPBS for 10 min, followed by rinsing with DPBS three times and blocking with 20% goat serum in DPBS for 90 min. The following primary antibodies, including mTOR rabbit monoclonal antibody (1:100), LAMP1 rat monoclonal antibody (1:200), and mouse monoclonal antibodies LAMP2 (1:100, Abcam, UK), PAX7 (1:300), and MyoD (1:100; Santa Cruz, USA), were incubated with the coverslips overnight at 4°C, followed by washing with PBST (0.1% Tween 20 in DPBS) three times for 5 min each time. Secondary antibodies, including goat anti-mouse IgG-Alexa Fluor 488 (1:200), goat anti-rat IgG-Alexa Fluor 488 (1:200), and goat anti-rabbit IgG-Alexa Fluor 594 (1:200; Invitrogen, USA), were incubated for 1 h at RT. Coverslips were mounted with in fluorescent mounting medium (Dako) with 0.1% DAPI and visualized with confocal fluorescence microscopy (LSM510, Zeiss, Germany) or (FV1000, Olympus, Japan). ImageJ and Image-Pro Plus software (USA) were used for quantification and co-localization analyses.

Histology

To examine the presence of CD3 T lymphocytes and macrophages in muscle tissues from treated *mdx* or control mice, muscle tissues were fixed in Bouin's solution (Sigma-Aldrich, USA) and embedded with paraffin. $CD3^+$ T lymphocytes or $CD68^+$ macrophages were stained with rabbit polyclonal antibodies CD3 (1:200) or CD68 (1:400, Abcam, UK) and detected by goat anti-rabbit secondary antibody (Sigma, USA). To measure the fibrotic areas, a Masson's trichrome staining kit (Sigma, USA) was applied as per the manufacturer's instructions. Routine H&E staining was used to examine the overall liver and kidney morphology and assess the level of infiltrating mononuclear cells. Quantification analysis was performed using ImageJ software.

Tissue Distribution

Lissamine-labeled PMO was diluted in 120 μL of saline or glycine and administered into adult *mdx* mice intravenously at 25 mg/kg/day for 3 days and tissues were harvested 4 days later. For the glycine-induction experiment, adult *mdx* mice were treated with 50 mg/mL glycine every other day for 1 week prior to single intravenous injection of FITC-labeled PMO at 50 mg/kg doses, and tissues were harvested 48 h later. Perfusion was performed with 50 mL of cold PBS to wash out free oligonucleotides in circulation. Body-wide muscles, liver, kidney, and brain were harvested for imaging and quantification with an *in vivo* imaging system (IVIS) (PerkinElmer, USA).

Generation of *RagB* Knockout HEK293T Cells

HEK293T cells were transfected with CRISPR/Cas9-expressing lentivirus (lentiviral CRISPR toolbox, Zhang Lab, USA), followed by 2 μg/mL blasticidin selection for 2 weeks. Cas9-expressing HEK293T cells were transfected with single guide RNA (sgRNA)-expressing lentivirus for 24 h, followed by 1 μg/mL puromycin selection for 2 weeks. The guide sequence targeting exon 3 of human *Rag*B is 5′- CCAC CACTAGGGGAACCGGA-3′.[62] The sgRNA was cloned into a lenti-Guide-Puro vector at the *Bsm*BI site as previously reported.[63]

RNA Extraction and RT-PCR analysis

Total RNA was extracted with TRIzol (Invitrogen, UK) as per the manufacturer's instructions. For the detection of PMO-mediated exon skipping of the murine *dmd* gene, 200 ng of RNA template was used for 20-mL RT-PCR with a One-Step RT-PCR kit (QIAGEN, UK), and nested RT-PCR was performed as described previously.[19] The products were examined by electrophoresis on a 2% agarose gel. For the validation of cell cycle-related gene expression, 1 μg of RNA as template was reverse transcribed into cDNA with a Transcriptor first-strand cDNA synthesis kit (Roche, Germany) per the manufacturer's instructions. Quantitative real-time PCR was performed with SYBR Green (Roche, Germany) on a 7500 Fast real-time PCR system (Applied Biosystems, USA). Primers used for the study were as follows: CCNE1, forward, 5′-CCTGCAGATGCTGTGCTCTAT-3′, reverse, 5′-CATCCCACATTTGCTCACAAC-3′; CDK1, forward, 5′-ACACCTTTCCCAAGTGGAAGC-3′, reverse, 5′-GCCATTTTGCCAGAGATTCG-3′; CDC20, forward, 5′-TTCCCAGGTGTGCTCCATCC-3′, reverse, 5′-CCCGTGCTGTGTGTCCTTTG-3′; CCNB1, forward, 5′-GCGTGTGCCTGTGACAGTTA-3′, reverse, 5′- CCTAGCGTTTTTGCTTCCCTT-3′; CCNB2, forward, 5′-TGTCAACAAGCAGCCGAAAC-3′, reverse, 5′-TCAGAGAAAGCTTGGCAGAGG-3′; CCNA1, forward, 5′-GCTGGCCATGAACTACCTG-3′, reverse, 5′-AGAGGCCACGAACATGC-3′; β-actin, forward, 5′-TGCACCACCAACTGCTTAG-3′, reverse, 5′-GGATGCAGGGATGATGTTC-3′. All quantitative real-time PCR data were performed with at least three biological replicates. The PCR products were confirmed by proper melting curves.

RNA Sequencing

Total RNA (3 μg/sample) was extracted from primary myoblasts isolated from *mdx* mice followed by incubation in 0.8 mM glycine for 24 h. RNA sequencing was performed as described previously.[64] Briefly, sequencing libraries were generated using an NEBNext Ultra RNA library prep kit for Illumina (NEB, USA) per the manufacturer's instructions, and index codes were added to attribute sequences to each sample. The clustering of the index-coded samples was performed on a cBot Cluster Generation System using TruSeq PE Cluster Kit v3-cBot-HS (Illumina, USA) according to the manufacturer's instructions. After cluster generation, the library preparations were sequenced on an Illumina HiSeq 2500 platform and 100-/50-bp single-end reads were generated. DESeq R package (1.10.1) was used for determining differential expression in digital gene expression data using a model based on the negative binomial distribution. A Benjamini-Hochberg approach was used to adjust the resulting p values for controlling the false discovery rate. Genes with an adjusted p value <0.05 were assigned as differentially expressed. A GOseq R package was used for Gene Ontology (GO) enrichment analysis of differentially expressed genes, in which gene length bias was corrected. GO terms with corrected $p < 0.05$ were considered significantly enriched by differentially expressed genes. Clustered heatmaps were produced by cluster 3.0 software. Original data were uploaded to Gene Expression Omnibus (GEO): GSE130843.

GLDC Knockdown in *mdx* Mice

For the *GLDC* knockdown experiment, three different shRNA target sequences were selected and optimized by Obio Technology (Shanghai, China). The selected *GLDC* shRNA was packaged in AAV2/8 serotype plasmid. High-titer AAV2/8 particles were produced and supplied by Obio Technology (Shanghai, China). AAV2/8 particles (40 μL) were injected into TA muscles of *mdx* mice, and the knockdown efficiency of GLDC protein was detected at 1 and 3 weeks post-injection. PMO (2 μg) in glycine was administered into the same TA muscles of *mdx* mice treated with *GLDC* shRNA 1 week after transduction and TA muscles were harvested 2 weeks after injection.

Isolation of Primary Myoblasts

Hindlimb muscles including gastrocnemius, quadriceps and TA were dissected and washed with pre-cooled D-Hanks buffer. All muscles were minced and digested with 400 U/mL type II collagenase (Sigma, USA) in D-Hanks buffer for 2 h at 37°C and centrifuged at 750 × *g* for 5 min. The digested fiber pellets were vortexed and filtered through 70-μm and 40-μm cell strainers, respectively, followed by centrifugation at 750 × *g* for 5 min and seeded in Matrigel-coated (1:100, Corning, USA) Petri dishes. Isolated primary myoblasts were cultured in Ham's F-10 (GIBCO, USA) supplemented with 20% FBS, 10% horse serum, 1% penicillin-streptomycin (GIBCO, USA), and 2.5 ng/mL bovine fibroblast growth factor (FGF) (PeproTech, USA). To examine the effect of glycine on isolated primary myoblasts, isolated primary myoblasts were cultured in growth medium supplemented with different concentrations of glycine in 96-well plates for 24 h, followed by cell counting with a hemocytometer.

Isolation of Satellite Cells

Hindlimb muscles were minced and digested with 250 U/mL type II collagenase (Sigma, USA) in D-Hanks buffer for 60 min at 37°C and then centrifuged at 750 × *g* for 5 min, followed by digestion with 60 U/mL type II collagenase and 3 U/mL type II dispase (Sigma, USA) for 45 min at 37°C. The digested fiber pellets were filtered through 70-μm and 40-μm cell strainers, respectively, and washed and then resuspended in D-Hanks buffer and immediately stained with anti-mouse antibodies, including PE (phycoerythrin)/VCAM (vascular cell adhesion molecule) (1:500), FITC/CD31 (1:500), FITC/CD45 (1:500), and allophycocyanin (APC)/Sca-1 (1:1,000, eBioscience, USA) for 30 min at 4°C, followed by analysis and sorting using the BD FACSAria II instrument (BD Biosciences, USA). For the isolation of satellite cells from skeletal muscle explants, it was adopted from previous reports.[65] Briefly, skeletal muscles isolated from hindlimbs were minced into small pieces and digested with 500 U/mL type II collagenase and 3 U/mL type II dispase in D-Hanks buffer for 60 min at 37°C, followed by centrifugation at 300 × *g* for 5 min. The fiber pellets were resuspended in high-glucose DMEM (GIBCO, USA) supplemented with 20% FBS, 10% horse serum, 1% penicillin-streptomycin, 1% antibiotic-antimitotic, and 2.5 ng/mL basic FGF (bFGF). The suspension containing small pieces of muscle tissues was seeded on Matrigel-coated flasks at 10%–20% surface coverage and incubated at 37°C and 5% CO_2 to allow attachment

of the tissues to the surface and subsequent migration of cells for 3–5 days. Cells from skeletal muscle explants were detached with 0.25% trypsin and centrifuged at 300 × *g* for 5 min. To separate the non-myogenic cells from myoblasts, cells were seeded on 0.2% gelatin-coated flasks and incubated at 37°C and 5% CO_2 for 1 h and the supernatant was transferred to a Matrigel-coated dish for subsequent culture.

Myoblast Transplantation in *mdx* Mice

CTX (2 μg) was injected into TA muscles of *mdx* mice and primary myoblasts (1×10^6) or muscle satellite cells (MuSCs) (1×10^5) were transplanted into the same injured TA muscle 1 day later as reported previously.[61] *Mdx* mice were fed with 7.5 mg/L FK506 (Astellas, Japan) in the drinking water every day during the experimental period as reported previously.[64,66] Glycine (120 μL) was intravenously injected into *mdx* mice every other day for 1 week prior to cell transplantation and continuously injected with the same dosing regimen during the experimental period. Treated *mdx* mice were monitored at week 1, 2, and 3 after transplantation with the IVIS imaging system (PerkinElmer, USA). TA muscles were harvested 3 weeks after transplantation and frozen in liquid nitrogen for storage.

Functional Grip Strength and Running Wheel Test

Treated and control mice were tested using a commercial grip strength monitor (Chatillon, West Sussex, UK) as described previously.[19] Briefly, each mouse was held 2 cm from the base of the tail, allowed to grip a protruding metal triangle bar attached to the apparatus with their forepaws, and pulled gently until they released their grip. The force exerted was recorded and five sequential tests were carried out for each mouse, averaged at 30 s apart. Subsequently, the readings for force recovery were normalized by the body weight. For muscle endurance, mice were placed in cages equipped with voluntary running wheels (Zhenhua, Anhui, China) in a quiet and clean room at a temperature of 24°C ± 1°C. Running circles were recorded and distance was analyzed.

Clinical Biochemistry

Serum and plasma were taken from the jugular vein immediately after killing with CO_2 inhalation. Analysis of serum creatinine kinase, AST, ALT, creatinine, and urea was performed by the clinical pathology laboratory (Tianjin Metabolic Disease Hospital, Tianjin, China).

Data Analysis

All data are reported as mean values ± SEM. Statistical differences between different treated groups were evaluated by SigmaStat (Systat Software, Chicago, IL, USA). Both parametric and non-parametric analyses were applied as specified in figure legends. Significance was determined based on $p < 0.05$.

Data and Materials Availability

All data needed to evaluate the conclusions in the paper are present in the paper and/or the Supplemental Information. Additional data related to this paper may be obtained from the corresponding author upon reasonable request.

SUPPLEMENTAL INFORMATION

Supplemental Information can be found online at https://doi.org/10.1016/j.ymthe.2020.03.003.

AUTHOR CONTRIBUTIONS

H.Y. conceived the project. C. L., G.H., and H.Y. designed the experiments, analyzed the data, and wrote the manuscript with input from all authors. C.L., G.H., H.N., J.S., and N.R. carried out the experiments. X.Y. and Y. S. performed the RNA sequencing data analysis.

CONFLICTS OF INTEREST

H.Y., C.L., and G.H. have filed a patent for glycine (application no. PCT/CN2019/109926). The authors declare no competing interests.

ACKNOWLEDGMENTS

The authors acknowledge Dr. Wenyan Niu (Tianjin Metabolic Disease Hospital, Tianjin Medical University, Tianjin, China) for assistance with the clinical biochemistry assays. This study was funded by National Key R&D Program of China (grant 2017YFC1001902); National Natural Science Foundation of China (grants 81802124 and 81672124); Postdoctoral Science Foundation of China (grant 2017M611176); Tianjin Municipal Science and Technology Key Project (grant 18JCQNJC79400); Tianjin Research Innovation Project for Postgraduate Students (grant 2019YJSB114); and Tianjin Municipal 13th Five-Year Plan (Tianjin Medical University Talent Project).

REFERENCES

1. Kaspar, R.W., Allen, H.D., Ray, W.C., Alvarez, C.E., Kissel, J.T., Pestronk, A., Weiss, R.B., Flanigan, K.M., Mendell, J.R., and Montanaro, F. (2009). Analysis of dystrophin deletion mutations predicts age of cardiomyopathy onset in Becker muscular dystrophy. Circ. Cardiovasc. Genet. *2*, 544–551.
2. Aartsma-Rus, A., and Krieg, A.M. (2017). FDA Approves eteplirsen for Duchenne muscular dystrophy: the next chapter in the eteplirsen saga. Nucleic Acid Ther. *27*, 1–3.
3. Mendell, J.R., Rodino-Klapac, L.R., Sahenk, Z., Roush, K., Bird, L., Lowes, L.P., Alfano, L., Gomez, A.M., Lewis, S., Kota, J., et al.; Eteplirsen Study Group (2013). Eteplirsen for the treatment of Duchenne muscular dystrophy. Ann. Neurol. *74*, 637–647.
4. Price, F.D., Kuroda, K., and Rudnicki, M.A. (2007). Stem cell based therapies to treat muscular dystrophy. Biochim. Biophys. Acta *1772*, 272–283.
5. Fujita, S., and Volpi, E. (2006). Amino acids and muscle loss with aging. J. Nutr. *136* (1, Suppl), 277S–280S.
6. Ham, D.J., Murphy, K.T., Chee, A., Lynch, G.S., and Koopman, R. (2014). Glycine administration attenuates skeletal muscle wasting in a mouse model of cancer cachexia. Clin. Nutr. *33*, 448–458.
7. Koopman, R., Ly, C.H., and Ryall, J.G. (2014). A metabolic link to skeletal muscle wasting and regeneration. Front. Physiol. *5*, 32.
8. Mok, E., Eléouet-Da Violante, C., Daubrosse, C., Gottrand, F., Rigal, O., Fontan, J.E., Cuisset, J.M., Guilhot, J., and Hankard, R. (2006). Oral glutamine and amino acid supplementation inhibit whole-body protein degradation in children with Duchenne muscular dystrophy. Am. J. Clin. Nutr. *83*, 823–828.
9. Hulmi, J.J., Lockwood, C.M., and Stout, J.R. (2010). Effect of protein/essential amino acids and resistance training on skeletal muscle hypertrophy: a case for whey protein. Nutr. Metab. (Lond.) *7*, 51.
10. Davoodi, J., Markert, C.D., Voelker, K.A., Hutson, S.M., and Grange, R.W. (2012). Nutrition strategies to improve physical capabilities in Duchenne muscular dystrophy. Phys. Med. Rehabil. Clin. N. Am. *23*, 187–199, xii–xiii.

11. Drummond, M.J., and Rasmussen, B.B. (2008). Leucine-enriched nutrients and the regulation of mammalian target of rapamycin signalling and human skeletal muscle protein synthesis. Curr. Opin. Clin. Nutr. Metab. Care *11*, 222–226.

12. Frost, R.A., and Lang, C.H. (2011). mTor signaling in skeletal muscle during sepsis and inflammation: where does it all go wrong? Physiology (Bethesda) *26*, 83–96.

13. Tan, H.W.S., Sim, A.Y.L., and Long, Y.C. (2017). Glutamine metabolism regulates autophagy-dependent mTORC1 reactivation during amino acid starvation. Nat. Commun. *8*, 338.

14. Saxton, R.A., and Sabatini, D.M. (2017). mTOR signaling in growth, metabolism, and disease. Cell *169*, 361–371.

15. Ham, D.J., Caldow, M.K., Lynch, G.S., and Koopman, R. (2014). Arginine protects muscle cells from wasting in vitro in an mTORC1-dependent and NO-independent manner. Amino Acids *46*, 2643–2652.

16. Razak, M.A., Begum, P.S., Viswanath, B., and Rajagopal, S. (2017). Multifarious beneficial effect of nonessential amino acid, glycine: a review. Oxid. Med. Cell. Longev. *2017*, 1716701.

17. Zhong, Z., Wheeler, M.D., Li, X., Froh, M., Schemmer, P., Yin, M., Bunzendaul, H., Bradford, B., and Lemasters, J.J. (2003). L-Glycine: a novel antiinflammatory, immunomodulatory, and cytoprotective agent. Curr. Opin. Clin. Nutr. Metab. Care *6*, 229–240.

18. Reinhold, J.G., and Kingsley, G.R. (1938). The chemical composition of voluntary muscle in muscle disease: a comparison of progressive muscular dystrophy with other diseases together with a study of effects of glycine and creatine therapy. J. Clin. Invest. *17*, 377–383.

19. Han, G., Gu, B., Cao, L., Gao, X., Wang, Q., Seow, Y., Zhang, N., Wood, M.J., and Yin, H. (2016). Hexose enhances oligonucleotide delivery and exon skipping in dystrophin-deficient *mdx* mice. Nat. Commun. *7*, 10981.

20. Ehmsen, J., Poon, E., and Davies, K. (2002). The dystrophin-associated protein complex. J. Cell Sci. *115*, 2801–2803.

21. Percy, M.E., Andrews, D.F., and Thompson, M.W. (1982). Serum creatine kinase in the detection of Duchenne muscular dystrophy carriers: effects of season and multiple testing. Muscle Nerve *5*, 58–64.

22. Kendall, G.C., Mokhonova, E.I., Moran, M., Sejbuk, N.E., Wang, D.W., Silva, O., Wang, R.T., Martinez, L., Lu, Q.L., Damoiseaux, R., et al. (2012). Dantrolene enhances antisense-mediated exon skipping in human and mouse models of Duchenne muscular dystrophy. Sci. Transl. Med. *4*, 164ra160.

23. Schiaffino, S., Rossi, A.C., Smerdu, V., Leinwand, L.A., and Reggiani, C. (2015). Developmental myosins: expression patterns and functional significance. Skelet. Muscle *5*, 22.

24. Aoki, Y., Nagata, T., Yokota, T., Nakamura, A., Wood, M.J., Partridge, T., and Takeda, S. (2013). Highly efficient in vivo delivery of PMO into regenerating myotubes and rescue in laminin-α2 chain-null congenital muscular dystrophy mice. Hum. Mol. Genet. *22*, 4914–4928.

25. Yin, H., Price, F., and Rudnicki, M.A. (2013). Satellite cells and the muscle stem cell niche. Physiol. Rev. *93*, 23–67.

26. McLoon, L.K., and Wirtschafter, J. (2003). Activated satellite cells in extraocular muscles of normal adult monkeys and humans. Invest. Ophthalmol. Vis. Sci. *44*, 1927–1932.

27. Harsing, L.G., Jr., Juranyi, Z., Gacsalyi, I., Tapolcsanyi, P., Czompa, A., and Matyus, P. (2006). Glycine transporter type-1 and its inhibitors. Curr. Med. Chem. *13*, 1017–1044.

28. Martin-Facklam, M., Pizzagalli, F., Zhou, Y., Ostrowitzki, S., Raymont, V., Brašić, J.R., Parkar, N., Umbricht, D., Dannals, R.F., Goldwater, R., and Wong, D.F. (2013). Glycine transporter type 1 occupancy by bitopertin: a positron emission tomography study in healthy volunteers. Neuropsychopharmacology *38*, 504–512.

29. Lamers, Y., Williamson, J., Theriaque, D.W., Shuster, J.J., Gilbert, L.R., Keeling, C., Stacpoole, P.W., and Gregory, J.F., 3rd (2009). Production of 1-carbon units from glycine is extensive in healthy men and women. J. Nutr. *139*, 666–671.

30. Ryall, J.G., Cliff, T., Dalton, S., and Sartorelli, V. (2015). Metabolic reprogramming of stem cell epigenetics. Cell Stem Cell *17*, 651–662.

31. Stover, P.J. (2009). One-carbon metabolism-genome interactions in folate-associated pathologies. J. Nutr. *139*, 2402–2405.

32. Albrecht, L.V., Bui, M.H., and De Robertis, E.M. (2019). Canonical Wnt is inhibited by targeting one-carbon metabolism through methotrexate or methionine deprivation. Proc. Natl. Acad. Sci. USA *116*, 2987–2995.

33. Brosnan, M.E., and Brosnan, J.T. (2016). Formate: the neglected member of one-carbon metabolism. Annu. Rev. Nutr. *36*, 369–388.

34. Ducker, G.S., and Rabinowitz, J.D. (2017). One-carbon metabolism in health and disease. Cell Metab. *25*, 27–42.

35. Douce, R., Bourguignon, J., Neuburger, M., and Rébeillé, F. (2001). The glycine decarboxylase system: a fascinating complex. Trends Plant Sci. *6*, 167–176.

36. Yoon, M.S. (2017). mTOR as a key regulator in maintaining skeletal muscle mass. Front. Physiol. *8*, 788.

37. Ruvinsky, I., and Meyuhas, O. (2006). Ribosomal protein S6 phosphorylation: from protein synthesis to cell size. Trends Biochem. Sci. *31*, 342–348.

38. Zeng, Z., Shi, Y.X., Tsao, T., Qiu, Y., Kornblau, S.M., Baggerly, K.A., Liu, W., Jessen, K., Liu, Y., Kantarjian, H., et al. (2012). Targeting of mTORC1/2 by the mTOR kinase inhibitor PP242 induces apoptosis in AML cells under conditions mimicking the bone marrow microenvironment. Blood *120*, 2679–2689.

39. Sun, K., Wu, Z., Ji, Y., and Wu, G. (2016). Glycine regulates protein turnover by activating protein kinase B/mammalian target of rapamycin and by inhibiting MuRF1 and atrogin-1 gene expression in C2C12 myoblasts. J. Nutr. *146*, 2461–2467.

40. Caldow, M.K., Ham, D.J., Trieu, J., Chung, J.D., Lynch, G.S., and Koopman, R. (2019). Glycine protects muscle cells from wasting *in vitro* via mTORC1 signaling. Front. Nutr. *6*, 172.

41. Sakata, K., Sato, K., Schloss, P., Betz, H., Shimada, S., and Tohyama, M. (1997). Characterization of glycine release mediated by glycine transporter 1 stably expressed in HEK-293 cells. Brain Res. Mol. Brain Res. *49*, 89–94.

42. Dilling, M.B., Germain, G.S., Dudkin, L., Jayaraman, A.L., Zhang, X., Harwood, F.C., and Houghton, P.J. (2002). 4E-binding proteins, the suppressors of eukaryotic initiation factor 4E, are down-regulated in cells with acquired or intrinsic resistance to rapamycin. J. Biol. Chem. *277*, 13907–13917.

43. Zoncu, R., Bar-Peled, L., Efeyan, A., Wang, S., Sancak, Y., and Sabatini, D.M. (2011). mTORC1 senses lysosomal amino acids through an inside-out mechanism that requires the vacuolar H^+-ATPase. Science *334*, 678–683.

44. Jensen, S.S., Aaberg-Jessen, C., Christensen, K.G., and Kristensen, B. (2013). Expression of the lysosomal-associated membrane protein-1 (LAMP-1) in astrocytomas. Int. J. Clin. Exp. Pathol. *6*, 1294–1305.

45. Yoshimori, T., Yamamoto, A., Moriyama, Y., Futai, M., and Tashiro, Y. (1991). Bafilomycin A1, a specific inhibitor of vacuolar-type H^+-ATPase, inhibits acidification and protein degradation in lysosomes of cultured cells. J. Biol. Chem. *266*, 17707–17712.

46. Sancak, Y., Bar-Peled, L., Zoncu, R., Markhard, A.L., Nada, S., and Sabatini, D.M. (2010). Ragulator-Rag complex targets mTORC1 to the lysosomal surface and is necessary for its activation by amino acids. Cell *141*, 290–303.

47. Garry, G.A., Antony, M.L., and Garry, D.J. (2016). Cardiotoxin induced injury and skeletal muscle regeneration. Methods Mol. Biol. *1460*, 61–71.

48. Schemmer, P., Bradford, B.U., Rose, M.L., Bunzendahl, H., Raleigh, J.A., Lemasters, J.J., and Thurman, R.G. (1999). Intravenous glycine improves survival in rat liver transplantation. Am. J. Physiol. *276*, G924–G932.

49. Wang, W., Wu, Z., Dai, Z., Yang, Y., Wang, J., and Wu, G. (2013). Glycine metabolism in animals and humans: implications for nutrition and health. Amino Acids *45*, 463–477.

50. Wu, B., Xiao, B., Cloer, C., Shaban, M., Sali, A., Lu, P., Li, J., Nagaraju, K., Xiao, X., and Lu, Q.L. (2011). One-year treatment of morpholino antisense oligomer improves skeletal and cardiac muscle functions in dystrophic mdx mice. Mol. Ther. *19*, 576–583.

51. Moulton, H.M., and Moulton, J.D. (2010). Morpholinos and their peptide conjugates: therapeutic promise and challenge for Duchenne muscular dystrophy. Biochim. Biophys. Acta *1798*, 2296–2303.

52. Pastoret, C., and Sebille, A. (1995). *mdx* mice show progressive weakness and muscle deterioration with age. J. Neurol. Sci. *129*, 97–105.

53. Ham, D.J., Gardner, A., Kennedy, T.L., Trieu, J., Naim, T., Chee, A., Alves, F.M., Caldow, M.K., Lynch, G.S., and Koopman, R. (2019). Glycine administration attenuates progression of dystrophic pathology in prednisolone-treated dystrophin/utrophin null mice. Sci. Rep. *9*, 12982.

54. Miller, R.A., Harrison, D.E., Astle, C.M., Bogue, M.A., Brind, J., Fernandez, E., Flurkey, K., Javors, M., Ladiges, W., Leeuwenburgh, C., et al. (2019). Glycine supplementation extends lifespan of male and female mice. Aging Cell *18*, e12953.

55. Shimobayashi, M., and Hall, M.N. (2016). Multiple amino acid sensing inputs to mTORC1. Cell Res. *26*, 7–20.

56. Bar-Peled, L., and Sabatini, D.M. (2014). Regulation of mTORC1 by amino acids. Trends Cell Biol. *24*, 400–406.

57. Emmert, M.Y., Fioretta, E.S., and Hoerstrup, S.P. (2017). Translational challenges in cardiovascular tissue engineering. J. Cardiovasc. Transl. Res. *10*, 139–149.

58. Weng, Q., Wang, J., Wang, J., Tan, B., Wang, J., Wang, H., Zheng, T., Lu, Q.R., Yang, B., and He, Q. (2017). Folate metabolism regulates oligodendrocyte survival and differentiation by modulating AMPKα activity. Sci. Rep. *7*, 1705.

59. Benoit, B., Meugnier, E., Castelli, M., Chanon, S., Vieille-Marchiset, A., Durand, C., Bendridi, N., Pesenti, S., Monternier, P.A., Durieux, A.C., et al. (2017). Fibroblast growth factor 19 regulates skeletal muscle mass and ameliorates muscle wasting in mice. Nat. Med. *23*, 990–996.

60. Fletcher, S., Honeyman, K., Fall, A.M., Harding, P.L., Johnsen, R.D., Steinhaus, J.P., Moulton, H.M., Iversen, P.L., and Wilton, S.D. (2007). Morpholino oligomer-mediated exon skipping averts the onset of dystrophic pathology in the mdx mouse. Mol. Ther. *15*, 1587–1592.

61. Zhang, H., Ryu, D., Wu, Y., Gariani, K., Wang, X., Luan, P., D'Amico, D., Ropelle, E.R., Lutolf, M.P., Aebersold, R., et al. (2016). NAD^+ repletion improves mitochondrial and stem cell function and enhances life span in mice. Science *352*, 1436–1443.

62. Jewell, J.L., Kim, Y.C., Russell, R.C., Yu, F.X., Park, H.W., Plouffe, S.W., Tagliabracci, V.S., and Guan, K.L. (2015). Differential regulation of mTORC1 by leucine and glutamine. Science *347*, 194–198.

63. Sanjana, N.E., Shalem, O., and Zhang, F. (2014). Improved vectors and genome-wide libraries for CRISPR screening. Nat. Methods *11*, 783–784.

64. Guo, Z., Jing, R., Rao, Q., Zhang, L., Gao, Y., Liu, F., Wang, X., Hui, L., and Yin, H. (2018). Immortalized common marmoset (*Callithrix jacchus*) hepatic progenitor cells possess bipotentiality in vitro and in vivo. Cell Discov. *4*, 23.

65. Shahini, A., Vydiam, K., Choudhury, D., Rajabian, N., Nguyen, T., Lei, P., and Andreadis, S.T. (2018). Efficient and high yield isolation of myoblasts from skeletal muscle. Stem Cell Res. (Amst.) *30*, 122–129.

66. Ilan, Y., Jona, V.K., Sengupta, K., Davidson, A., Horwitz, M.S., Roy-Chowdhury, N., and Roy-Chowdhury, J. (1997). Transient immunosuppression with FK506 permits long-term expression of therapeutic genes introduced into the liver using recombinant adenoviruses in the rat. Hepatology *26*, 949–956.

YMTHE, Volume *28*

Supplemental Information

Glycine Enhances Satellite Cell Proliferation, Cell Transplantation, and Oligonucleotide Efficacy in Dystrophic Muscle

Caorui Lin, Gang Han, Hanhan Ning, Jun Song, Ning Ran, Xianfu Yi, Yiqi Seow, and HaiFang Yin

Supplementary Figures

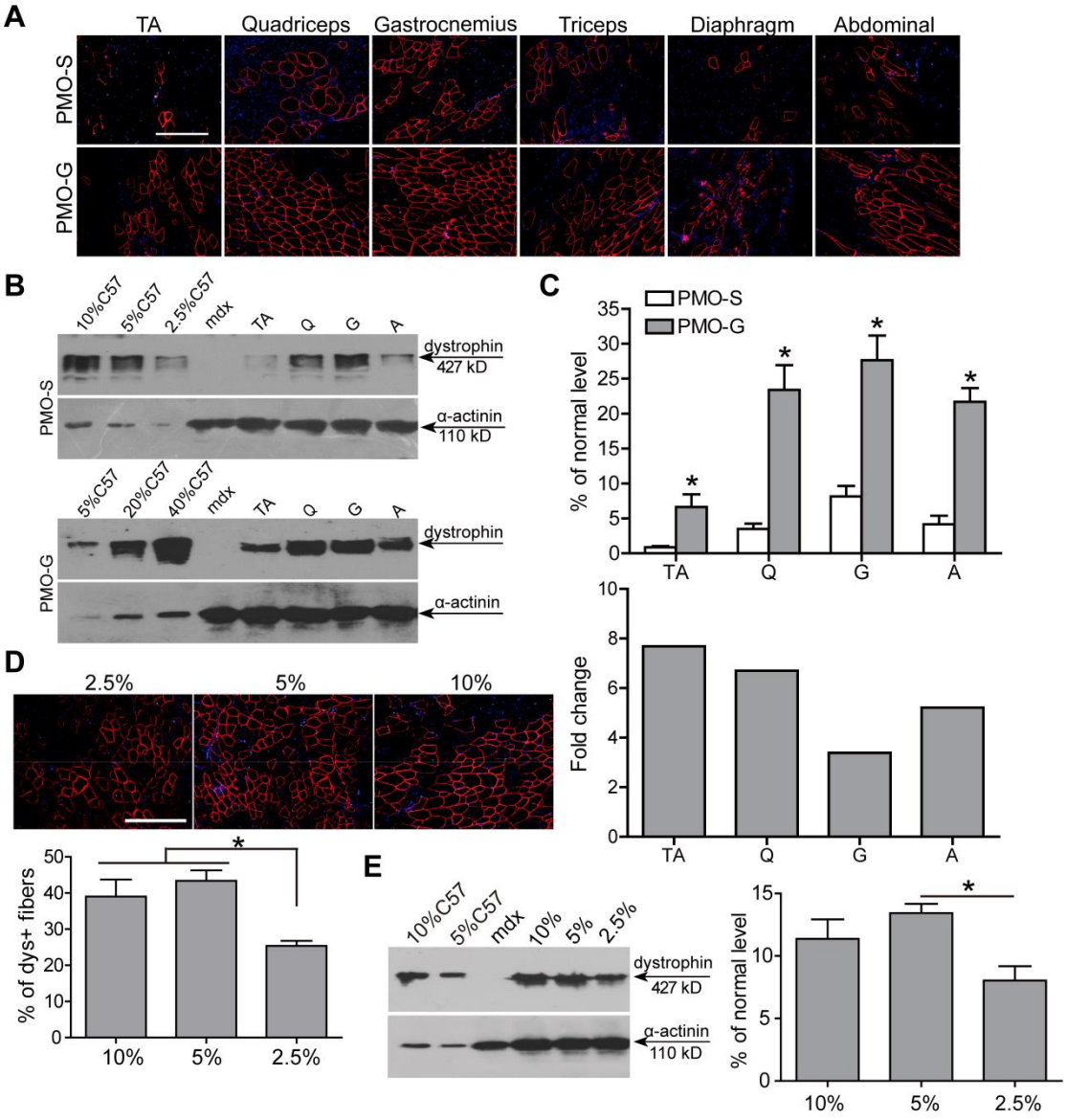

Supplementary Figure 1. Systemic evaluation of glycine with PMO at 50 mg/kg dose and local test of different concentrations of glycine with PMO in *mdx* mice. PMO in glycine or saline was administered intravenously into adult *mdx* mice at 50 mg/kg/week for 3 weeks and muscles were harvested 2 weeks after last injection. (**A**) Immunohistochemistry for dystrophin-positive fibers in body-wide muscles from *mdx* mice treated with PMO in saline (PMO-S) or glycine (PMO-G) at 50 mg/kg/week for 3 weeks intravenously (scale bar=100 μm). Western blot (**B**) and quantitative analysis (**C**) for dystrophin expression in body-wide muscles from *mdx* mice treated with PMO-G or PMO-S at 50 mg/kg/week for 3 weeks intravenously (n=3; two-tailed t test). 1.25 μg, 2.5 μg, 5 μg, 10 μg and 20 μg total protein from *C57BL/6* and 50 μg muscle samples from untreated and treated *mdx* mice were loaded. α-actinin was used as the loading control. The fold change refers to PMO-G relative to PMO-S. TA-tibialis anterior, Q-quadriceps, G-gastrocnemius, A-abdominal muscle. (**D**)

Immunohistochemistry and quantitative analysis of dystrophin-positive fibers in TA muscles from *mdx* mice treated with single intramuscular injection of PMO in different concentrations of glycine (scale bar=100 μm) (n=3; One way -ANOVA post hoc Student-Newman-Keuls test). PMO (2 μg) in different concentrations of glycine was administered into TA muscles of adult *mdx* mice. (**E**) Western blot and quantitative analysis for dystrophin expression in TA muscles from *mdx* mice treated with single intramuscular injection of PMO in different concentrations of glycine (n=3; One way-ANOVA post hoc Student- Newman-Keuls test). 2.5 μg and 5 μg total protein from *C57BL/6* and 50 μg of muscle samples from untreated and treated *mdx* mice were loaded. Data are presented as means ±s.e.m. (*$p<0.05$).

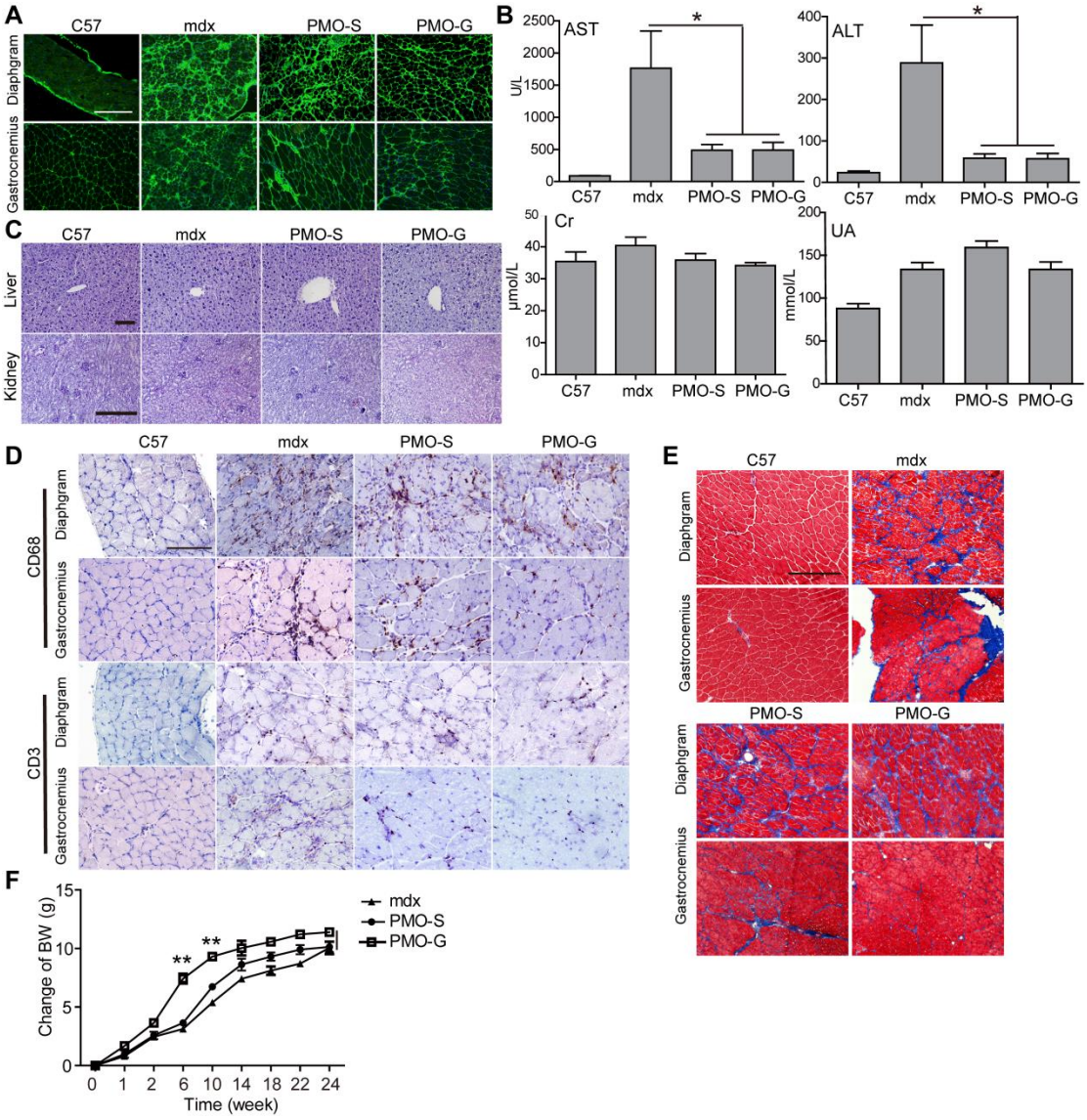

Supplementary Figure 2. Pathological and toxicological assessment of *mdx* mice treated with long-term repeated administration of PMO-G at 25 mg/kg. PMO-G was administered intravenously into adult *mdx* mice at 25 mg/kg/week for 3 weeks with additional supply of glycine every other day, followed by 50 mg/kg/month for 5 months with additional supply of glycine every one week intravenously. Muscles were harvested 2 weeks after last injection. (**A**) Immunohistochemistry for IgGs in gastrocnemius and diaphragm from *mdx* mice treated with PMO-S or PMO-G (scale bar=100 μm). (**B**) Measurement of serum indices from treated *mdx* mice to reflect liver and kidney functions (n=4; One way -ANOVA post hoc Student -Newman-Keuls test). (**C**) Morphological examination of liver and kidney from treated *mdx* mice (scale bar=50 μm). (**D**) Immunohistochemistry of immune cells in gastrocnemius and diaphragm from treated *mdx* mice (scale bar=50 μm). (**E**) Masson Trichrome staining for gastrocnemius and diaphragm from treated *mdx* mice (scale bar=100 μm). (**F**) Measurement of body-weight changes of treated *mdx* mice (n=4; One way -ANOVA post hoc Student-Newman-Keuls test). Data are presented as means ±s.e.m. (*p<0.05; **p<0.001).

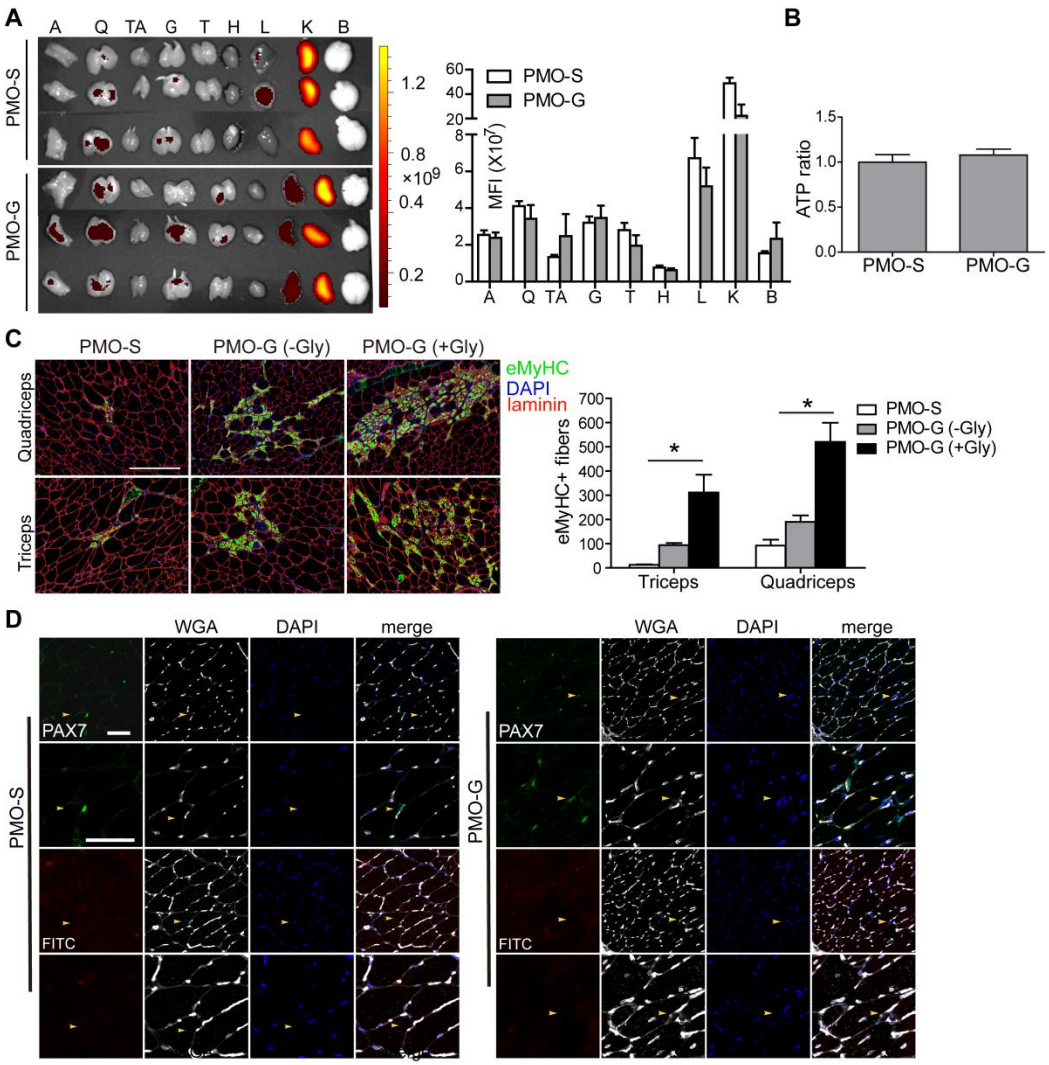

Supplementary Figure 3. Investigation of the mechanism underlying glycine's functionality in *mdx* mice. (**A**) Tissue imaging to examine the fluorescence of lissamine-labelled PMO in body-wide tissues of treated *mdx* mice. Adult *mdx* mice were treated with lissamine-labelled PMO in glycine or saline at 25 mg/kg/day for 3 days intravenously and tissues were harvested 4 days later (n=3). (**B**) Measurement of ATP levels in quadriceps from *mdx* mice treated with PMO-G or PMO-S at 25 mg/kg/week for 3 weeks (n=3). (**C**) Immunohistochemistry and quantitative analysis for eMyHC^{+} regenerating myofibres in quadriceps and triceps from treated *mdx* mice (scale bar=100 μm) (n=4, *P<0.05; One way-ANOVA post hoc Student-Newman-Keuls test). Adult *mdx* mice were treated with PMO-G with additional glycine injections (+Gly) or without additional glycine (-Gly) at 25 mg/kg/week for 3 weeks and glycine was administered every other day intravenously. (**D**) Immunohistochemistry of PAX7^{+} MuSCs and FITC-labelled PMO in gastrocnemius from treated *mdx* mice (scale bar=50 μm). *Mdx* mice were treated with single intravenous injection of FITC-labelled PMO in glycine (PMO-G) or saline (PMO-S) at the dose of 50 mg/ kg and muscles were harvested 48 hr later. Fluorescently tagged wheat germ agglutinin (WGA) was used for the visualization of connective tissues. Data are presented as means ±s.e.m.

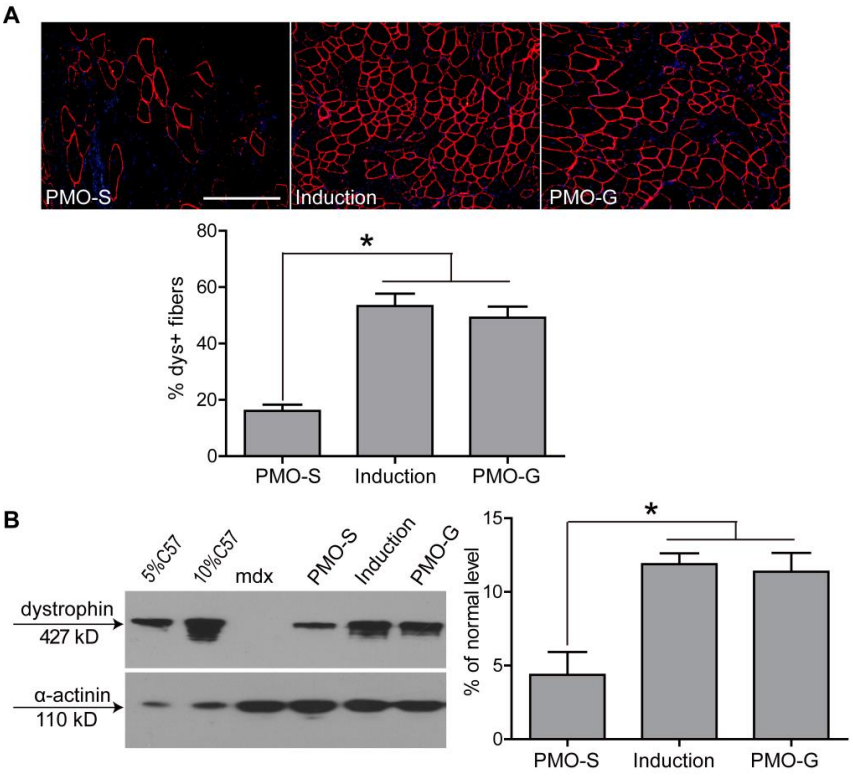

Supplementary Figure 4. **Effect of glycine pre-treatment on PMO activities in TA muscles of adult *mdx* mice.** Glycine (5%) was intramuscularly injected into TA muscle of adult *mdx* mice for once and followed by administration of PMO (2 μg) in saline into the same TA muscles 3 days later. TA muscles were harvested 10 days after PMO injection. (**A**) Immunohistochemistry and quantitative analysis for dystrophin-positive fibers in *mdx* TA muscles treated with PMO in saline (PMO-S), PMO in glycine (PMO-G) and glycine induction (induction) (scale bar=100 μm) (n=3, *P<0.05; One way-ANOVA post hoc Student-Newman-Keuls test). (**B**) Representative Western blot and quantitative analysis for dystrophin expression in TA muscles from treated *mdx* mice (n=3, *P<0.05; One way -ANOVA post hoc Student-Newman-Keuls test). 2.5 μg and 5 μg total protein from *C57BL/6* and 50 μg of muscle samples from untreated and treated *mdx* mice were loaded. α-actinin was used as the loading control. Data are presented as means ±s.e.m.

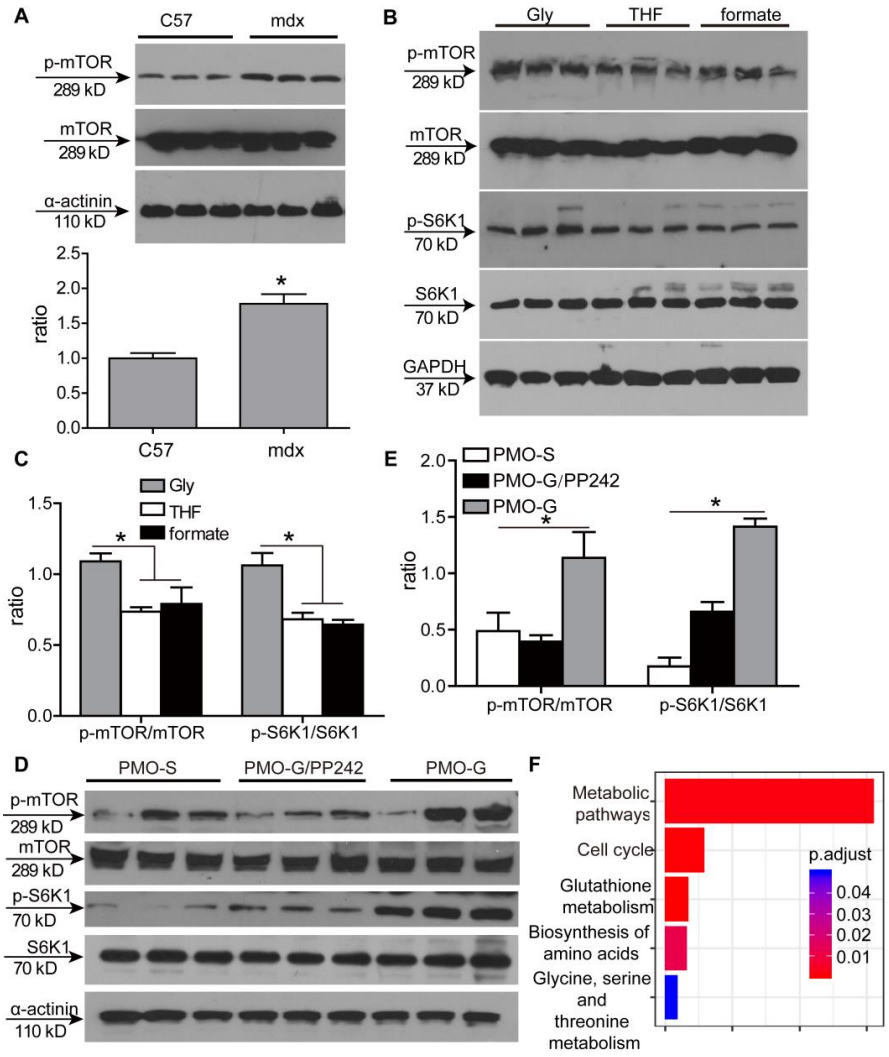

Supplementary Figure 5. Examination on the mTORC1 signaling pathway in *C57BL/6*, untreated and treated *mdx* mice. (**A**) Western blot to detect phosphorylated mTOR expression in TA muscles from *C57BL/6* and *mdx* mice (n=3; two-tailed t test). α-actinin was used as the loading control. 70 μg total protein were loaded. (**B**) Western blot to detect phosphorylated mTOR and S6K1 expression in TA muscles from *mdx* mice treated with glycine, THF or formate intramuscularly. GAPDH was used as the loading control. 50 μg total protein were loaded. (**C**) Quantitative analysis of the ratio of phosphorylated mTOR and S6K1 to total mTOR and S6K1 expression, respectively (n=3; One way -ANOVA post hoc Student-Newman-Keuls test). (**D**) Western blot to detect phosphorylated mTOR and S6K1 expression in TA muscles from *mdx* mice treated with PMO-S, PMO-G or PMO in the mixture of glycine and PP242 (PMO-G/PP242) intramuscularly. α-actinin was used as the loading control. 50 μg total protein were loaded. (**E**) Quantitative analysis of the ratio of phosphorylated mTOR and S6K1 to total mTOR and S6K1 expression, respectively (n=3; One way -ANOVA post hoc Student-Newman-Keuls test). (**F**) Gene set enrichment analysis (GSEA) of metabolism and cell cycle-related genes for primary myoblasts isolated from *mdx* mice followed by treatment with 0.8mM glycine for 24 hr (n=6). The number of biological replicates in the control group is 3 (n=3). Data are presented as means ±s.e.m. (*$p<0.05$).

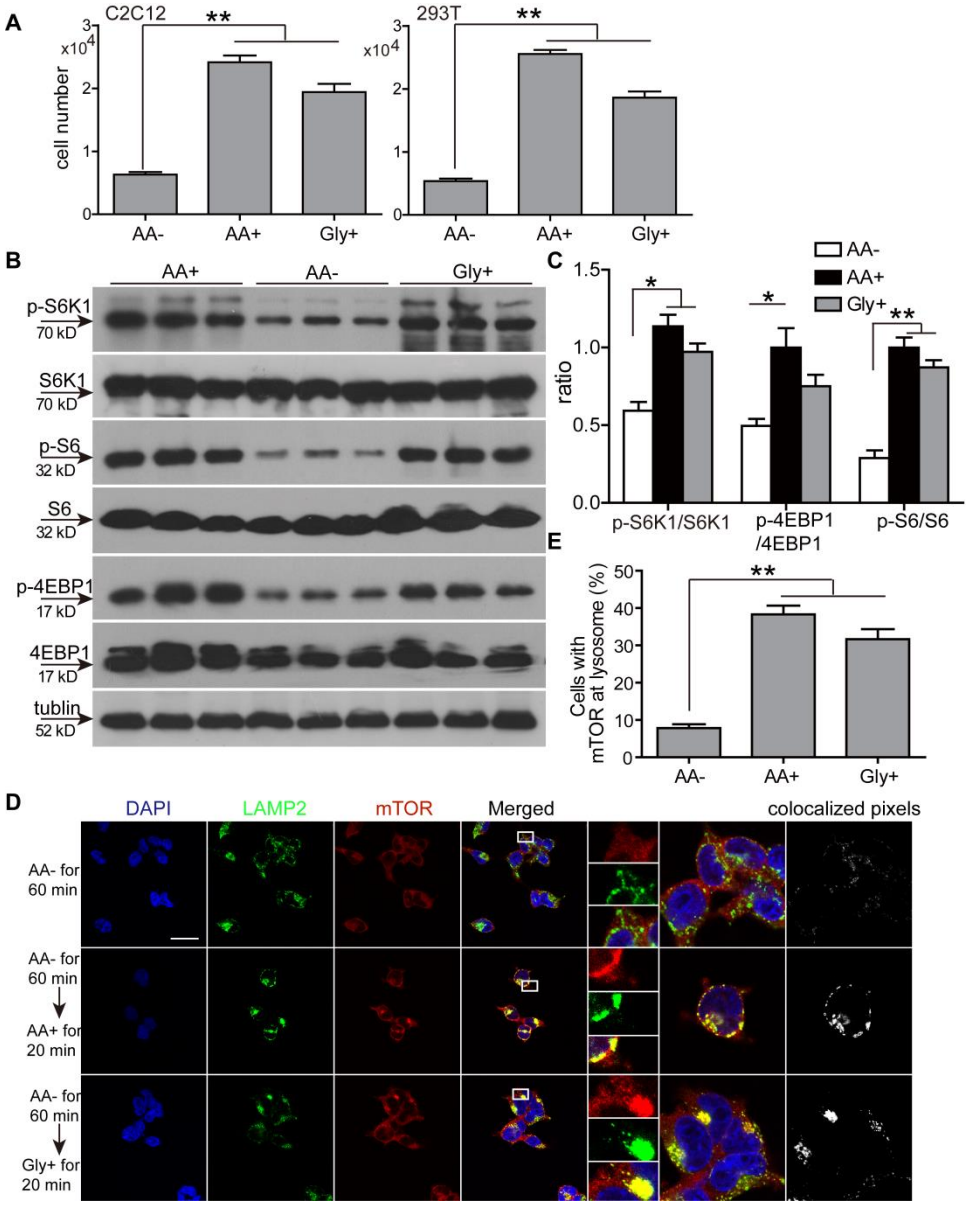

Supplementary Figure 6. Glycine enhances activation of the mTOR signaling pathway in 293T cells. (**A**) Measurement of cell growth in starved C2C12 and 293T cells followed by re-stimulation of glycine and total amino acid (n=4; One way -ANOVA post hoc Student-Newman-Keuls test). AA- means the depletion of total amino acid; AA+ or Gly+ refers to the supplementation of total amino acid and glycine into starved cells. (**B**) Western blot to detect phosphorylated S6K1, S6 and 4EBP1 expression in 293T cells under different conditions. 30 μg total protein was loaded and tubulin was used as a loading control. (**C**) Quantitative analysis of the ratio of phosphorylated S6K1, S6 and 4EBP1 to total protein expression of counterparts (n=3; One way -ANOVA post hoc Student- Newman-Keuls test). Immunocytochemistry for mTOR (**D**) and quantitative analysis of cells with mTOR at lysosomes (**E**) in starved 293T cells followed by re-stimulation of total amino acid or glycine (scale bar=10 μm) (n=10; One way -ANOVA post hoc Student-Newman-Keuls test). LAMP2 was used as a lysosome marker. Data are presented as means ±s.e.m. (*p<0.05; **p<0.001).

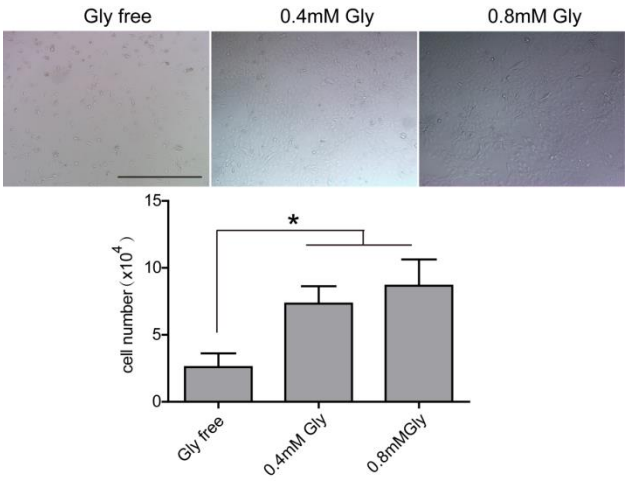

Supplementary Figure 7. Measurement of the effect of glycine on murine primary myoblasts. Primary myoblasts were isolated from wild-type *C57BL/6* mice and cultured for 24 hrs with different concentration of glycine (scale bar=100μm) (n=4, *P<0. 05; One way -ANOVA post hoc Student-Newman-Keuls test). Data are presented as means ±s.e.m.

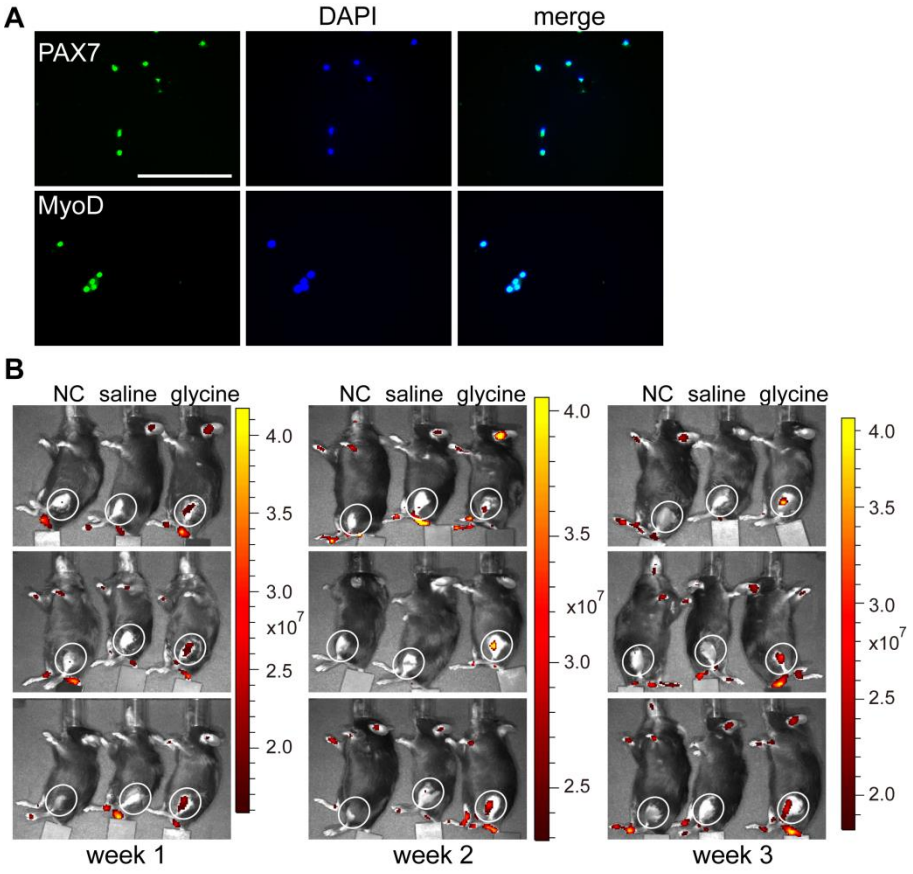

Supplementary Figure 8. Immunocytochemistry for isolated MuSCs from transgenic GFP *C57BL/6* mice (A) and real-time monitoring of transplanted GFP-positive MuSCs in TA muscles of adult *mdx* mice (B). *Mdx* mice were imaged for GFP fluorescence at different time-points after cell transplantation (n=3).